Effect of processing temperature profile during melt extrusion on thermoplastic starch production

Miguel Aldas[1], Cristina Pavon[2,*], Harrison De La Rosa-Ramírez[2], Juan López-Martínez[2] and Marina P. Arrieta[3,4]

[1] Departamento de Ciencia de Alimentos y Biotecnología, Facultad de Ingeniería Química y Agroindustria, Escuela Politécnica Nacional (EPN), 170517 Quito, Ecuador. (M.A. miguel.aldas@epn.edu.ec, ORCID: 0000-0003-3491-6618)

[2] Instituto Universitario de Tecnología de Materiales, Universitat Politècnica de València (UPV), 03801 Alcoy-Alicante, Spain. (C.P. cripava1@epsa.upv.es ORCID: 0000-0003-2902-0059, H.R.R. hardela@epsa.upv.es ORCID: 0000-0002-2913-7938, J.L-M. jlopezm@mcm.upv.es ORCID: 0000-0001-6904-2282)

[3] Departamento Ingeniería Química Industrial y del Medio Ambiente, Universidad Politécnica de Madrid, E.T.S.I. Industriales, 28006 Madrid, Spain. (M.P.A. m.arrieta@upm.es, ORCID: 0000-0003-1816-011X)

[4] Grupo de Investigación: Polímeros, Caracterización y Aplicaciones (POLCA), 28006 Madrid, Spain

***Correspondence:**

Cristina Pavon (cripava1@epsa.upv.es) (C.P.)

Laboratorio F3L5, Universitat Politècnica de València, Instituto Tecnológico de Materiales.

Campus Alcoy, Plaza Ferrándiz y Carbonell N°1, 03801 Alcoy (Alicante), Spain.

ABSTRACT

This work aims to evaluate the influence of the processing temperature on thermoplastic starch (TPS) for scalable production at the industrial level. Thus, it analyses the impact of six different extruding temperature profiles to plasticize native starch with water as well as with glycerol to obtain thermoplastic starch (TPS) produced by melt-extrusion. The temperature profiles ranged from 70 to 150 ºC. At temperature profiles below 100 ºC, the extrusion conditions were insufficient to disrupt the starch granules completely. Therefore, the material did not plasticize correctly, and the starchy matrix plasticizes partially using a temperature profile of 100 ºC. The water evaporation process affects the final material's microstructure. At temperature profiles above 100 ºC (i.e., 110 and 130ºC), the extrusion conditions allowed the disruption of the starch granule as well as a good material plasticization to obtain TPS. Although TPS obtained with a temperature profile of 150 ºC displayed the highest mechanical properties, the material shows signs of thermal degradation under these conditions. Therefore, TPS processed at a profile with a maximum temperature of 130 ºC showed a higher plasticization effect, good thermal and mechanical properties, and good water uptake capability. With its potential for successful industrial production, TPS can be obtained by processing native starch with water and glycerol at low share rates of 20 rpm and using 130ºC as a maximum processing temperature, offering a range of benefits.

Keywords: thermoplastic starch, temperature profile, extrusion, plasticization, retrogradation

3.1.1. INTRODUCTION

Bio-based and biodegradable materials play an essential role in helping conserve the environment, replacing non-degradable synthetic plastics with more friendly alternatives that could reduce the accumulation of plastic garbage due to lack of degradation or poor waste management (Ruhul Amin et al., 2020). Bio-based materials such as biofibers, bio-composites, and bioplastics are an alternative to synthetic plastics in different industrial products, mainly in short-term applications or disposable products such as the case of plastic bags, disposables (i.e., plates, cups, cutlery, and straws), food packaging or agricultural mulch films (Vinod et al., 2020). In this regard, the European Commission specified that where sustainable alternatives are effortlessly accessible and affordable, single-use plastic products cannot be used (European Commission, 2023). Even though the European Commission encourages the use of recycled plastic in single-use products, the present legislation establishes stringent requests regarding food safety and for food contact materials does not permit the direct use of recycled plastics coming from recycled streams (European Commission, 2022). Therefore, fully biobased and biodegradable plastics can be used in single-use products directly interacting with food. Consequently, the production of food contact materials based on bioplastics is increasing. In this regard, bioplastics are materials produced from biomass, agro-resources, microorganisms, or synthesized from bioderived monomers (Vinod et al., 2020), for instance: cellulose (Gopi, Balakrishnan, et al., 2019; Gopi, Pius, et al., 2019; Rayón et al., 2013), alginates (Farokhi et al., 2019), proteins such as casein or caseinates (Arrieta et al., 2013), and starch (Aldas et al., 2021; Nevoralová et al., 2019; Pavon et al., 2021).

Although still substantially less than traditional plastics, the current biopolymer worldwide production is about 2.18 million tons (European bioplastics, 2023), and 18.7% of the total bioplastic production comes from starch (European Bioplastics, 2021) and the packaging sector is the largest market segment for bioplastics (with 43 % of the total bioplastics market in 2023). Therefore, starch seems to be one of the most promising bioplastics for outspreading bioplastics applications in food packaging and disposables. Starch is usually used as raw material for the development of biopolymer formulations as it is abundant in nature, inexpensive, comes from renewable sources, and due to its

intrinsic biocompatible and biodegradable character (Ismail et al., 2017; Jiménez et al., 2012; X. Zhang et al., 2022). In general, bioplastics based on starch are used as blends with biodegradable polyesters (Ferri et al., 2018; Pattanayaiying et al., 2019), with synthetic polymers to add a grade of sustainability to the final formulation as it is biobased and compostable (Sessini et al., 2019), as a matrix in biocomposites (Hassan et al., 2019; Jung et al., 2019; Rabe et al., 2019), and also in coatings and packaging developments (Arrieta et al., 2017; Gadhave et al., 2018). Additionally, there are commercial starch bioplastics such as Mater-Bi from Novamont, Bioplast from Biotec, Eslon Green, and Greenpol from Yukong LTD (Bastioli, 1998; Mitrus & Wojtowicz, Agnieszka Moscicki, 2009), which have been blended with other natural additives to modify their properties (Aldas et al., 2019; Aldas, Rayón, et al., 2020; Scaffaro et al., 2018; X. Zhang et al., 2022).

Starch is a natural biopolymer synthesized by plants and some cyanobacteria whose primary function is to store carbohydrates in spherical granules, whose size, quantity, and composition vary depending on the species that produce it (Apriyanto et al., 2022; Jiménez et al., 2012). The most common starch sources are cereal grains, such as barley, oats, and wheat; corn or potatoes; and cassava tubers (Jumaidin et al., 2020). Structurally, starch is a semicrystalline polymer made up of two D-glucose homopolymers: amylose, usually a linear polymer with α (1 → 4) linkages, and amylopectin, with α (1 → 6) linkages, which are highly branched (Apriyanto et al., 2022; Bertoft, 2017; Iaccheri et al., 2023). The content of amylose and amylopectin in the starch structure depends on various factors, such as the source of origin, age, or the extraction technique of the granules. A common starch has amylose contents between 20 % and 25 % and amylopectin contents between 75 % and 80 % (Marichelvam et al., 2019). In its native state, starch is found as solid, insoluble granules, so for its processing, it is required to transform the granule to a fluid state (Xie et al., 2014). As reviewed by Jiménez *et al.* (2012), starch has mainly been investigated for developing edible and biodegradable films using the film formation method by solvent casting (Jiménez et al., 2012). Nevertheless, for its industrial uses, starch must be transformed into thermoplastic starch (TPS), a polymeric material based on a starchy matrix that interests the plastic processing industry. Since starch degradation temperature is inferior to starch melting temperature, to obtain a TPS, starch requires the action of heat and shear forces in addition to the incorporation of a plasticizer such as water, glycerol, or sorbitol (Xie et al., 2014; Y. Zhang, Rempel, & McLaren, 2014). As already commented, solvent-casting can obtain TPS at a laboratory level. However, for its industrial use, TPS can be processed using identical techniques employed for processing conventional polymeric systems, like extrusion or injection molding. (Aldas, Pavon, et al., 2020b; Jumaidin et al., 2020; Mitrus, 2009; Oniszczuk & Janssen, 2009) It is expected that with the replacement of petrol-based materials for more sustainable solutions, the processing conditions for TPS-based materials at the industrial scale would improve. In obtaining TPS at an industrial scale level, it should be considered that plasticizers are used to decrease the starch melting temperature and help destroy its crystalline structure. In its natural state, starch has a crystalline structure that can hinder its processing. The addition of plasticizers disrupts this structure, making the starch more amorphous and easier to process. (Montilla-Buitrago et al., 2021). It is worth mentioning that water helps to plasticize starch and prevents starch degradation during melt extrusion (Mitrus, 2009; Montilla-Buitrago et al., 2021). When the starch heats up with a plasticizer, gelatinization occurs, which involves granule swelling, followed by a disruption of the crystal structure that will lead to the starch melting. (H. Ma et al., 2022; Xie et al., 2014). On the other hand, shear forces, apart from producing a homogeneous blend, also cause the destructuration of the crystal structure. In addition, they can physically break the granules to allow plasticizers to enter the starch structure, affecting the final performance of the thermoplastic material (Xie et al., 2012). Thus, heating, shear forces, and plasticizers contribute to the starch melting process, successfully leading to TPS formation (Jumaidin et al., 2020).

Another factor to consider for the industrial production of TPS is that the temperature and the shear forces applied during melt extrusion can degrade the material (Wilpiszewska & Spychaj, 2006; Ye et

al., 2018). The degradation degree will depend on a more significant measure of the processing parameters, for instance, the temperature profile used during the extrusion process and the rotation speed of the screws. Still, it also will depend on the composition and moisture content present in the material (Wilpiszewska & Spychaj, 2006; Xie et al., 2012). Although many authors stated that the processing conditions are of fundamental importance in TPS production for its scalable manufacture because they can considerably affect the final performance of the starchy material, including the temperature profile and the moisture content (Toro-Márquez et al., 2018), there are no studies on the obtained properties of TPS-based materials as affected by different processing temperatures which are of fundamental importance for the plastic processing industry.

The existing literature related to TPS extrusion processing focuses more on the study of the plasticizer's influence on the material properties (Montilla-Buitrago et al., 2021; Schmitt et al., 2015a; Yunos & Rahman, 2011; X. Zhang et al., 2022) and the impact of the extrusion variables (i.e., L/D ratio, shear force, rotational speed, among others) (Artz et al., 1990; Souza & Andrade, 2002a; Thuwall et al., 2006; Ye et al., 2018), not on the temperature influence. These studies used glycerol extensively as a plasticizer because of its availability, low cost, and high boiling point (290 ºC) (Kaseem et al., 2012). In this regard, it is well known that glycerol and water are suitable plasticizers because of their small molecular size, allowing them to enter the three-dimensional structure of starch easily (Montilla-Buitrago et al., 2021; Y. Zhang, Rempel, & Liu, 2014). Additionally, glycerol is a by-product of the biodiesel manufacturing process, and its use as a plasticizer allows the revalorization of a low-grade by-product, contributing to a circular economy (Arrieta et al., 2013). Corn starch is the type of starch most used for TPS elaboration due to its high availability around the world (Ciardelli et al., 2019), and since its high amylose content helps both in the starch gelatinization and the enhancement of the tensile properties of the biopolymers obtained, concerning TPS produced from low amylose starches (Marichelvam et al., 2019). However, it is worth mentioning that Enrione et al. (2010) studied the glass transition temperature (T_g) of different sources of thermoplastic starches and no significant differences were observed in the glass transition temperature between extruded rice starches and waxy maize, nonetheless at high contents of glycerol did form glycerol-rich zones in these polymeric systems which could affect the overall T_g of TPS (Enrione et al., 2010). Therefore, the glycerol plasticizer should be homogeneously distributed into the starchy matrix to achieve an excellent thermoplastic material.

As was previously commented, with the new legislation, the production of TPS-based polymeric formulations is increasing in the industrial sector. Even more, research regarding TPS production via thermoplastic extrusion is gaining significant interest in the revalorization of wastes to obtain starch and promote new starch sources of thermoplastic starch. Costa et al. (2022) used modified loquat seed starch as a non-conventional source of starch to produce films for food contact applications, and the obtained films seemed to be attractive for low and medium water content foodstuff as kinds of pasta and baked food (Costa et al., 2022). Romeira et al. (2021) used potato starch acquired from potato-washing slurries produced by a Food Company. They revalorized it, preparing thermoplastic starch films with an adequate cost and a potential application in film-forming solution for its use as papaya fruit coating (Romeira et al., 2021). Moro et al. (2017) mixed the residues of the passion fruit juice industry with starch in the film-forming process by thermoplastic extrusion. The researchers found that the residue added in 4 % enhanced the mechanical strength and Young’s modulus and decreased the water vapor permeability (Moro et al., 2017). Therefore, to extend the applications of TPS-based products at the industrial level, understanding the effect of processing temperature on the final overall performance of TPS-based materials is of fundamental importance.

Even though the processing temperature is a fundamental parameter to achieving gelatinization and granules melting of starch, few published studies address the influence of different extrusion temperatures on TPS's overall performance. It should be appropriately studied as TPS production and

use rapidly increase for single-use food contact materials applications. Among them is a work done by Schmitt et al. in 2015, which analyzes the effect of different plasticizers over the retrogradation of thermoplastic starch. Even though the study analyses four different extrusion temperature profiles on TPS processing, 110–115–115 °C, 90–90–110 °C, 105–110–110 °C and 105–110–110 °C, each temperature profile was used for processing a different material with different plasticizers: 110–115–115 °C for water and glycerol, 90–90–110 °C for sorbitol, and 105–110–110 °C for glycerol/sorbitol as well as urea/ethanolamine blend. As the primary objective of these studies was to analyze the effects of the used plasticizer, the temperature profile was not isolated, and there is no more profound analysis of the temperature profile used (Schmitt et al., 2015b) and thus, no deeper analysis on the effect of the processing temperature on the TPS performance. Pushpadass et al. 2008 studied the effect of extrusion temperature on TPS processing. However, the study assessed only two temperatures (110 °C and 120 °C). Furthermore, this parameter is not isolated since changes in TPS composition with different plasticizers were also analyzed (stearic acid, urea, and sucrose). Thus, the study only concludes that TPS's physical and functional properties depend primarily on the type of plasticizer without a clear conclusion on the processing temperature (Pushpadass et al., 2008).

On the other hand, literature reports a wide range of TPS processing temperatures (from hopper to die) used by different authors for TPS production. For instance, Schmitt et al. (2015) work with wheat starch and blends of various plasticizers (i.e., glycerol or sorbitol, as well as a blend of glycerol/sorbitol, or urea/ethanolamine blend), and in this work, different temperature profiles of 110--115-115 °C; 90-90-110 °C; 105110-110 °C and 105-110-110 °C were used with an screw speed of 60 rpm (Schmitt et al., 2015a). Ghanbari et al. (2018) processed TPS from corn starch and glycerol with an extrusion speed of 80 rpm under the temperature profile of 80-100-110-115-120 °C-125 °C (Ghanbari et al., 2018). Mitrus (2005) studied TPS with potato starch and glycerol, and they used an extrusion temperature profile from 75 to 140 °C and a speed from 60 to 100 rpm (Mitrus, 2005). Wang and Huang (2007) processed TPS from corn starch using glycerol and ethanolamine as plasticizers, and they used a temperature profile of 110-115-120-125 °C and a speed of 20 rpm (Wang & Huang, 2007a). Souza and Andrade (2002) processed corn starch and glycerol with an extrusion speed from 20 to 40 rpm and a temperature profile of 70-80-95-115 °C (Souza & Andrade, 2002b). Liu et al. (2010) used a temperature profile of 50-80-140 °C and a rotation speed of 180 rpm when working with corn starch, glycerol, and water (Liu et al., 2010).

Van Soest et al. (1996) worked with a rising and falling temperature profile of 85-140-145-120-80-95 °C and an extrusion screw speed of 55 rpm. The final temperature was below 95 °C to prevent water from boiling and obtain a non-porous material (Van Soest et al., 1996). In brief, most temperature profiles established for processing TPS are in rising order, with a gradual increase in temperature. In most cases, the intervals are between 5 and 10 °C to avoid undesired effects such as changes in viscosity and degradation rate, which temperature variations could produce during extrusion (Liu et al., 2010). While it seems that the use of different temperature profiles will affect the overall performance of the TPS, there are no deep analyses of the effect of this processing parameter on the structure and overall performance of the obtained TPS.

In most cases, the temperature processing conditions are determined from previously reported experiences and by trial-and-error practice during the processing of the materials until good-quality TPS samples are obtained. Therefore, a deeper study on the effect of different processing temperatures is still needed to extend TPS production from the laboratory scale to the industrial level and its massive applications in single-use plastics. This study intends to fill the gaps in deeper analyses of the influence of the processing temperature profile on the general performance of TPS obtained from corn starch and further plasticized with water and glycerol by the melt extrusion process intended for sustainable food packaging applications. Glycerol was selected as it is food grade and the most used plasticizer for TPS production at the industrial level. This study uses a screw speed of 20 rpm to

ensure that starch degradation due to high shear does take place, while the mixing time was 5 min. Then, six TPS-based formulations were prepared by melt extrusion using six different maximum processing temperatures of 70 ºC, 90 ºC, 100 ºC, 110 ºC, 130 ºC, and 150 ºC. The obtained formulations were characterized to get insights on the effect of processing temperature on the obtention and the performance of TPS for their scalable production in the industrial sector. Thus, the paper analyzes obtained TPS's morphology, structural, mechanical, thermal, transparency, and UV-blocking properties as affected by the processing temperature used to get information regarding the industrial processing conditions to extend the TPS commercial applications in the food packaging field. Additionally, as the moisture gain in materials intended for food contact applications is a critical issue, surface wettability and water absorption measurements were also conducted. This work determined the optimal temperature profile and made recommendations to understand the processability of TPS made with starch, glycerol, and water in which the hydroxyl groups of glycerol destroy the original hydrogen bonds previously established in starch molecules between them and allow to obtain starchy matrix in its thermoplastic form showing it potential industrial scalability.

1. MATERIALS AND METHODS

1.1. Materials

Food-grade corn starch composed of 27% amylose, provided by Cargill (Barcelona, Spain), was used to elaborate TPS. Glycerol with a purity of 99% provided by Panreac (Barcelona, Spain) and distilled water were used as plasticizers. Glycerol was added at 25 wt.% and water at 10 wt.% of the total blend. Then, the materials were manually premixed in an airtight polyethylene bag. They were stored for 24 hours to ensure the plasticizers, water, and glycerol entrance into the starch granules (Oniszczuk & Janssen, 2009).

1.2. Thermoplastic starch processing

Before extrusion, the blend was stirred to guarantee material homogeneity and regular feeding (Oniszczuk & Janssen, 2009). The blend was processed at 20 rpm using a co-rotating twin-screw extruder with an L/D ratio 25 from Dupra S.L. (Castalla, Spain). Five different temperature profiles were used to study the influence of processing temperature on the overall performance of TPS, which varied in steps of 20 °C between each profile. In addition, a temperature profile at 100 °C was used to verify the behavior of TPS at the water boiling temperature. The samples were labeled according to the maximum temperature used in the processing profile. Table 1 lists the labels with corresponding extrusion profiles.

Table 1. Label of the TPS studied materials according to the extrusion temperature profile

Sample label	Extrusion temperature profile (ºC)			
	Zone 1 (Die)	Zone 2	Zone 3	Zone 4 (Feeding hopper)
T70	70	60	50	40
T90	90	80	70	60
T100	100	90	80	70
T110	110	100	90	80
T130	130	120	110	100
T150	150	140	130	120

The die of the extruder was a round sheet with holes of a diameter of 3.5 mm. The extrusion process allowed filaments with diameters between 3 and 4.5 mm to be obtained. The filaments undergo the

respective characterization. Meanwhile, to determine the transparency, UV-blocking effect, and surface wettability, the obtained filaments were pelletized and processed into films at 10 ºC higher than the maximum temperature used in the processing profile for each film (i.e., for T70 80ºC, for T90 100ºC, for T100 110ºC, for T110 120ºC, for T130 140ºC, and T150 160°C) in a hot press (WTPR-20, MrHide). The pellets were kept between the plates at atmospheric pressure for 4 min until melting, then to the following pressure profiles: 3 MPa for 1 min, 5 MPa for 1 min, 10 MPa for 1 min, and 30 MPa for 2 min. Then, films were quenched at room temperature at atmospheric pressure. Since the environmental conditions influence TPS-based materials' properties, the obtained starchy samples were kept at 25 ℃ and 50 ± 5% HR immediately after extrusion and before being characterized (Aldas et al., 2019).

1.3. Thermoplastic starch characterization

1.3.1. Visual and optical characterization

Visual and color characterization evaluated the obtained filaments' color, surface appearance, and diameter. The visual and optical examination of the filaments evaluates their appearance. The optical examination uses an Olympus optical microscope, model SZX7 from Olympus Iberia (Barcelona, Spain), and a digital microscopic camera to photograph the filaments. Filamnet's diameters were measured with an electronic digital caliper, model Pro-Max, from Fowler High Precision (Newton, Massachusetts, USA). The color was measured on a Colorflex-Diff2 458/08 colorimeter from HunterLab (Reston, VA, USA) using the CIEL*a*b* space by determining L *, a *, and b * coefficients. The average of ten measurements determined color and sample diameter. The results report the mean values with the corresponding standard deviation.

The significant differences were statistically analyzed with the one-way analysis of variance (ANOVA), using OriginPro 8 software, at a 95% confidence level according to Tukey's test for the significant differences among starchy samples.

UV-visible transmittances of the samples analyzed the transparency of the TPS-based materials through processed into films in the 800-250 nm region by using a Varian Cary 1E UV-Vis spectrophotometer (Varian, USA) equipped with an integrating sphere and using a scanning speed of 400 mm/min. The film samples were of 1 cm × 3 cm shapes to fit the measuring cell.

1.3.2. Microstructural characterization

Field Emission Scanning Microscopy (FESEM) was carried out on a Zeiss Ultra 55 microscope at 1 kV over the surface of the filaments. Before the analysis, the obtained filaments were cryo-fractured and covered with a layer of gold-palladium alloy using a Sputter Mod Coater Emitech SC7620, Quorum Technologies (East Sussex, UK) to allow electrical conduction.

X-ray Diffraction (XRD) studied the crystallinity variations in the thermoplastic starch structure due to the changes in the processing temperature profile. A Bruker D8 Advance X-Ray Diffractometer with a linear detector Lynxeye XE allowed the X-ray Diffraction patterns to be obtained. The experiment used scattering angles (2θ) from 4° to 50° at a rate of 1°/min. The measurements used a 1 mm thick sample with a smooth surface.

Attenuated total reflectance–Fourier transform infrared spectroscopy (FTIR-ATR) was employed to analyze the molecular interactions of TPS components and their changes due to the processing

temperature profile. The analysis runs at ambient temperature in transmission mode in a Nicolet iS10 FTIR spectrometer (Thermo Scientific, Waltham, MA, USA) coupled with a Smart iTX ATR accessory. The experimental wavenumber range was within 4000–600 cm^{-1}, the resolution was 16 cm^{-1}, and 16 scans were performed.

1.3.3. Mechanical characterization

Tensile test measurements were carried out on an Ibertest Elib 30 SAE Ibertest (Madrid, Spain) universal testing machine following ISO 527 standard (International Standards Organization, 2012), with a 5 kN load cell and 10 mm/min speed. The tensile test used extruded filament samples of 80 ± 1 mm length and constant diameter as test specimens with a grip distance of 50 mm.

The average of five measurements determined Young's modulus, tensile strength, and elongation at break. The area under the stress-strain curve was calculated using the OriginPro2015 program to determine the TPS's toughness. The mean value and the standard deviation for each sample are reported. The significant differences in the measurements were calculated using the same parameters previously described.

1.3.4. Thermal characterization

Thermogravimetric analysis (TGA) was conducted on a TGA Q500 TA Instruments thermal analyzer (Selb, Germany). A dynamical analysis was carried out from 35 °C to 700 °C with a heating rate of 10 °C/min using nitrogen with a 30 mL/min flow rate as circulating gas. The onset decomposition temperature was determined when the materials lost 5% of their weight ($T_{5\%}$). The end decomposition temperature is when the materials lose 90% of their initial weight ($T_{90\%}$). The maximum decomposition rate temperature (T_{max}) was determined at the minimum of the first derivative of the TGA curve (DTG).

Differential scanning calorimetry (DSC) was conducted on Mettler DSC821e equipment (Toledo, Spain). The samples were analyzed using a dynamic thermal cycle consisting of a heating step from -50 °C to 170 °C, followed by a cooling step to -50 °C, and second heating from - 50 °C to 170 °C. The speed was 10 °C/min in all the steps, and the circulating atmosphere air was nitrogen (flow of 30 mL/min). The second heating curves were used to obtain the transition temperatures (T_g).

Dynamic mechanical thermal analysis (DMTA) was conducted in DMA1 Mettler-Toledo (Schwerzenbach, Switzerland) using filaments of constant diameter as samples. The analysis was carried out using a single cantilever mode and a maximum deformation of 10 μm. The samples were analyzed within −100 up to 100 °C with a heating rate of 2 °C/min and a frequency of 1 Hz.

1.3.5. Water contact angle

The surface wettability of films was studied by measuring the water contact angle (WCA) using an Ossila Contact Angle Goniometer equipped with a high-resolution camera and analysis software. The WCA followed the UNE: EN ISO 828:2013 standard (International Standards Organization, 2013) by randomly adding at least five drops of distilled water (20 μL) with a syringe to the films' surfaces at room temperature and measuring the contact angle after 10 s of the water drop deposition.

1.3.6. Water uptake

The water uptake test followed ISO 62 standards (International Standards Organization, 2008). extruded filament specimens of 25 ± 1 mm length and constant diameter were the samples in the test. The initial weight (W_1) was determined by drying the samples at 50 °C for 48 h. Then, each sample was placed in a container with 300 mL of distilled water at room temperature. The samples were weighed every 15 min during the first hour, then every 30 min until 3 hours of testing, and every hour until 8 hours of testing to plot the change in sample weight evolution over time due to water absorption. For each measurement, the specimens were removed from the flasks, the surface was wiped out with filter paper, and weighed again (W2). The water absorption (c) at each point was determined with Equation 1. Three specimens of each material were tested. The mean values were reported with their corresponding standard deviation, and the significant differences were statistically calculated with the same parameters previously mentioned.

$$c = \frac{W_2 - W_1}{W_1} \times 100 \quad (1)$$

2. RESULTS

2.1. Thermoplastic starch formulations, processing, and visual characterization

It is known that starch can exhibit thermoplastic properties when processed with plasticizers, applied shear, and at elevated temperatures. In the present work, glycerol was selected as a plasticizer as it is the most widely used plasticizer for TPS production at the industrial level. It is a food-grade product obtained as a by-product during biodiesel manufacturing. Therefore, from a circular economy point of view, using glycerol as a plasticizer increases its added value from a low-grade by-product to a plasticizer for sustainable biopolymeric formulation production (Arrieta et al., 2013). Moreover, glycerol and water are considered the most effective plasticizers for TPS production mainly because of their small size as well as their hydrophilic nature, which make them compatible with the starch matrix, allowing ease of penetration within the three-dimensional starch networks (Pushpadass et al., 2008).

The percentages of glycerol and water were established in this work according to the literature because TPS production widely uses glycerol. In this sense, Oniszczuk and Janssen. (2009) have proven that 25 wt.% of glycerol is enough to complete starch gelatinization. While minor contents that are more than 25 wt.%, do not produce a complete plasticization, with higher contents, a migration of glycerol occurs (Oniszczuk & Janssen, 2009). Furthermore, the researchers added water at 10 wt.% since Liu et al. (2010) showed that adding water to the blend aided the gelatinization and prevented the degradation of the starch granules (Liu et al., 2010; Y. Zhang, Rempel, & Liu, 2014). To avoid thermomechanical degradation of TPS polymer in the melt extrusion, since starch degradation temperature is lower than its melting temperature, not only the temperature profile should be carefully selected, but also screw speed as well as mixing time.

In this work, before processing, the materials were manually premixed in sealed plastic bags and then allowed to rest for 24 hours to promote the entrance of plasticizers, water, and glycerol. The obtained swelled mixtures of starch, glycerol, and water were then fed into the extruder and processed at a screw speed of 20 rpm to avoid starch degradation due to high shears. Fig 1 and Table 2 present the appearance of the different filaments obtained and the optical micrographs, respectively.

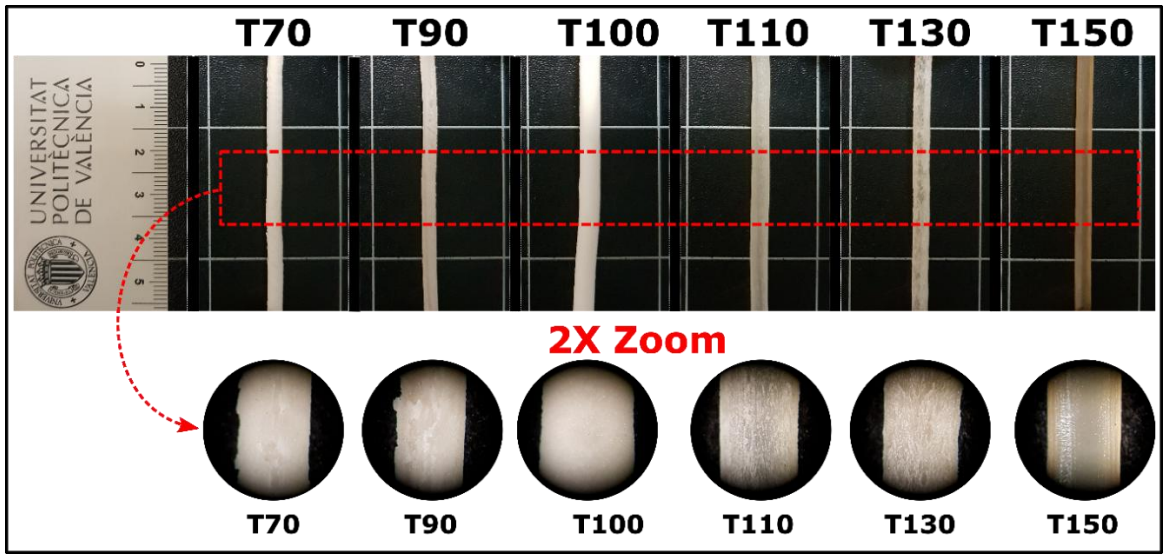

Fig 1 Visual appearance and microscopic view (1.6X) of TPS filaments obtained at different temperatures at a screw speed of 20 rpm

Table 2. Visual characterization results of the obtained filaments

Sample label	Filament diameter (mm)	Superficial appearance	Color			
			L*	a*	b*	YI
T70	3.2±0.1[a]	Matte, rough, heterogeneous surface with scales and opaque.	73.0±1.1[a]	0.4±0.1[a]	9.4±0.5[a]	22.7±1.1[a]
T90	3.1±0.1[a]	Matte, rough, heterogeneous, and opaque surface with scales.	63.6±0.6[b]	0.8±0.1[a]	9.5±0.2[a]	26.0±0.7[b]
T100	4.4±0.1[b]	Matte, smooth, homogeneous, and opaque surface.	81.3±1.8[c]	-0.7±0.1[b]	9.6±0.4[a]	18.6±0.4[c]
T110	3.7±0.1[c]	Matte, rough, homogeneous, and translucent surface.	46.4±0.6[d]	-1.7±0.2[c]	7.9±0.6[b]	24.8±1.3[a,b]
T130	3.5±0.1[d]	Matte, rough, homogeneous, and translucent surface with scales	51.1±1.1[e]	-0.5±0.8[b]	8.7±0.4[a,b]	25.3±2.0[b]
T150	3.6±0.1[d]	Shiny, smooth, homogeneous, and translucent surface.	32.9±0.6[f]	2.5±0.2[d]	12.2±0.7[c]	55.4±1.3[d]

[a–f] Different letters within the same property indicate statistically significant differences between materials ($p < 0.05$).

The diameters of the filaments processed at low (T70, T90) and high temperatures (T130 and T150, respectively) do not show significant differences among them ($p > 0.05$). The filaments processed below 100 °C have a smaller diameter than those processed at 100 ºC or higher temperatures. Also, the filament processed at 100 °C presents the largest diameter of all the studied materials (4.4 ± 0.1 mm). This behavior is because, at this temperature, the water in the blend evaporates just as the filament leaves the extruder, which causes the swelling of the material. Therefore, the diameter increases, as was observed by Mitrus (Mitrus, 2009). Regarding the surface appearance of the filament and the color, the processed materials at temperatures below 100 °C (T70 and T90) present a heterogeneous surface, which suggests a poor and heterogeneous plasticization of the starch matrix (Fig 1 and Table 2). There is also a color change in these filaments. For the T100 material, the L* coordinate, which indicates the material luminosity, is 81.3 ±1.8, so the filament is seen in white tones. This change in color and the smooth appearance of the filament are due to water evaporation. For T130, the luminosity shows a reduction on the L* coordinate concerning T100, but it is

significantly higher than T100, suggesting intermediate lightness between these two samples. Meanwhile, the color is mainly similar to that of T110 since they showed similar values of b* coordinate and YI ($p > 0.05$), indicating a trend to a certain degree to yellow. However, in the case of T150 materials, which represent the highest temperature used here, the smooth appearance of the surface may suggest the beginning of a degradation process due to the high processing temperature used, corroborated by the color change. This sample's coordinates, a* and b*, tend to have higher positive values, so the material displays a brown hue. In addition, the yellowing index increases significantly ($p < 0.05$) from YI = 25 (in the previous processing temperature of 130) to YI = 55 (in T150), suggesting that the material suffered thermal degradation during processing. Finally, a reduction in the L* value shows a loss of clarity (luminescence), suggesting a starch recrystallization.

In food packaging, transparency is a vital consumer requirement when looking at the packed food. Therefore, a light transmission analysis was performed in the visible and UV regions in the films of the materials. Fig 2 shows the transparency results obtained by UV-Vis assessment. Results show that formulations extruded at T100, T110, and T130 maximum profile temperatures have the highest transparency. These results show that starch granules break down completely, creating a plasticized TPS and, therefore, one-phase materials (as shown in FESEM micrographs, Fig 3). These microstructures confer higher transparency to the materials. When processing TPS with the maximum profile temperatures below 100 °C (T70 and T90), the incomplete disruption of the starchy granule generates two-phase materials (broken and unbroken granules), as further shown in FESEM micrographs (Fig 3), and thus, the transparency decreases. At the T150 as the maximum temperature profile, crystalline structures reappear in the TPS-based formulation due to the recrystallization process, leading to a two-phase microstructure and decreasing the transparency of this material.

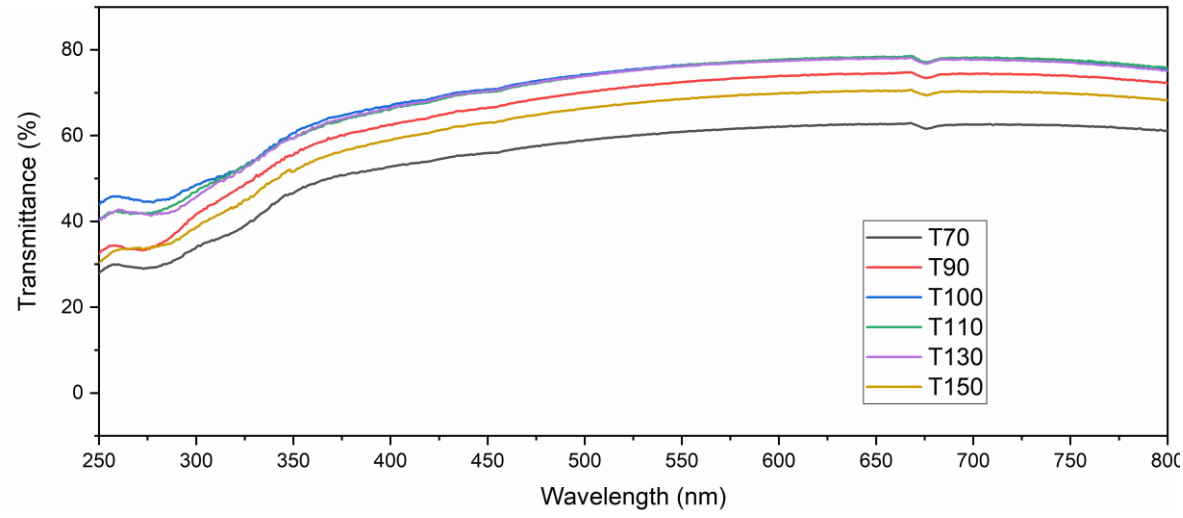

Fig 2. Transmittance percentage of light in the range of 250 to 800 nm for TPS obtained at different processing temperature profiles.

Regarding the UV spectra region (250-400 nm), although in all the TPS-based materials, the UV-B (280 to 315 nm) and UV-A (400 to 315 nm) light passes through the film, there is a reduction of the light transmission on the UV-C region (280-100 nm), usually produced by artificial light sources, showing that TPS transmits less UV-C light than LDPE (Auras et al., 2004).

2.2. Microstructural characterization

Fig 3 displays the morphological changes on the TPS matrix due to the different processing temperatures. Fig 3-a shows the corn starch granules, whose morphology and size (between 5 and 12 µm) agree with that reported in the literature (Wilpiszewska & Spychaj, 2006; Xie et al., 2014; Y. Zhang, Rempel, & Liu, 2014). T70 and T90 (Fig 3-b and Fig 3-c) presented two phases within the same material, a continuous phase formed by the plasticized starch granules and a dispersed phase consisting of whole or partially broken starch granules (X. Ma & Yu, 2004; Yang et al., 2006; Zullo & Iannace, 2009). The unbroken granules show that the maximum temperatures of 70 ºC and 90 ºC, used in the temperature profiles for processing T70 and T90, respectively, are not enough to disrupt the starchy granule completely. Therefore, the plasticizer cannot fully enter the starch granular structure, which does not allow the transformation process from starch to TPS to be completed (Xie et al., 2012).

On the other hand, T100 (Fig 3-d) displays a porous structure produced by the boiling and evaporation of water contained in the initial TPS formulation (Mitrus, 2009). Meanwhile, T110 (Fig 3-e) presents a ductile fracture surface with a few holes, suggesting the presence of starch granule residues. Thus, the images indicate that T100 and T110 structures are partially plasticized. Quite the opposite, T130 (Fig 3-f) presents a smooth and soft surface where starch granules cannot be distinguished, showing a material free of defects. Arredondo-Ochoa et al. (2017), studied edible films of oxidized corn-starch plasticized with sorbitol prepared by solvent casting method and observed a similar compact structure (Arredondo Ochoa et al., 2017). In the current work, the homogeneous material obtained at this temperature (T130 ºC) indicates a good combination of temperature and shear force in the extrusion process, allowing a better granule disruption (Zullo & Iannace, 2009). In this way, a strong interaction between starch, glycerol, and water occurs, producing adequate material plasticization at a maximum temperature of 130ºC Similar findings were observed by Ma and Yu, who prepared formamide/glycerol plasticized TPS (X. Ma & Yu, 2004). However, although amide groups have shown their effectiveness in plasticizing starchy matrices as a consequence of the electronegativity of their functional groups, they are not permitted for food contact materials due to their toxicity (Montilla-Buitrago et al., 2021).

T150 (Fig 3-g) exhibited new structures on the material surface (expanded area Fig 3-g,) which could be ascribed to thermal degradation due to the high temperature during the extrusion process. Thermal degradation mainly affects amylopectin molecules (Stepto, 2006a; Xie et al., 2014). In this condition, the amylopectin chains interact among them, which causes recrystallization on cooling, resulting in a more rigid and crystalline structure (Hoover, 2001; Paridah et al., 2016). Furthermore, the high temperatures to which T150 is subjected may break the amylose chains, facilitating a rearrangement of the chains upon cooling (Y. Zhang, Rempel, & Liu, 2014). Additionally, the material color change previously commented on (see T150 in Fig 1) suggests that thermal degradation had taken place in T150, which confirms the retrogradation (recrystallization) phenomenon (Paridah et al., 2016; Stepto, 2006b). Other works also observed these crystalline structures when studying a Mater-Bi type bioplastic, a commercial thermoplastic based on a thermoplastic starch matrix widely used in the bioplastic processing industry (Aldas, Rayón, et al., 2020). The cracks observed on the surface may have resulted from the cryofracture of the sample.

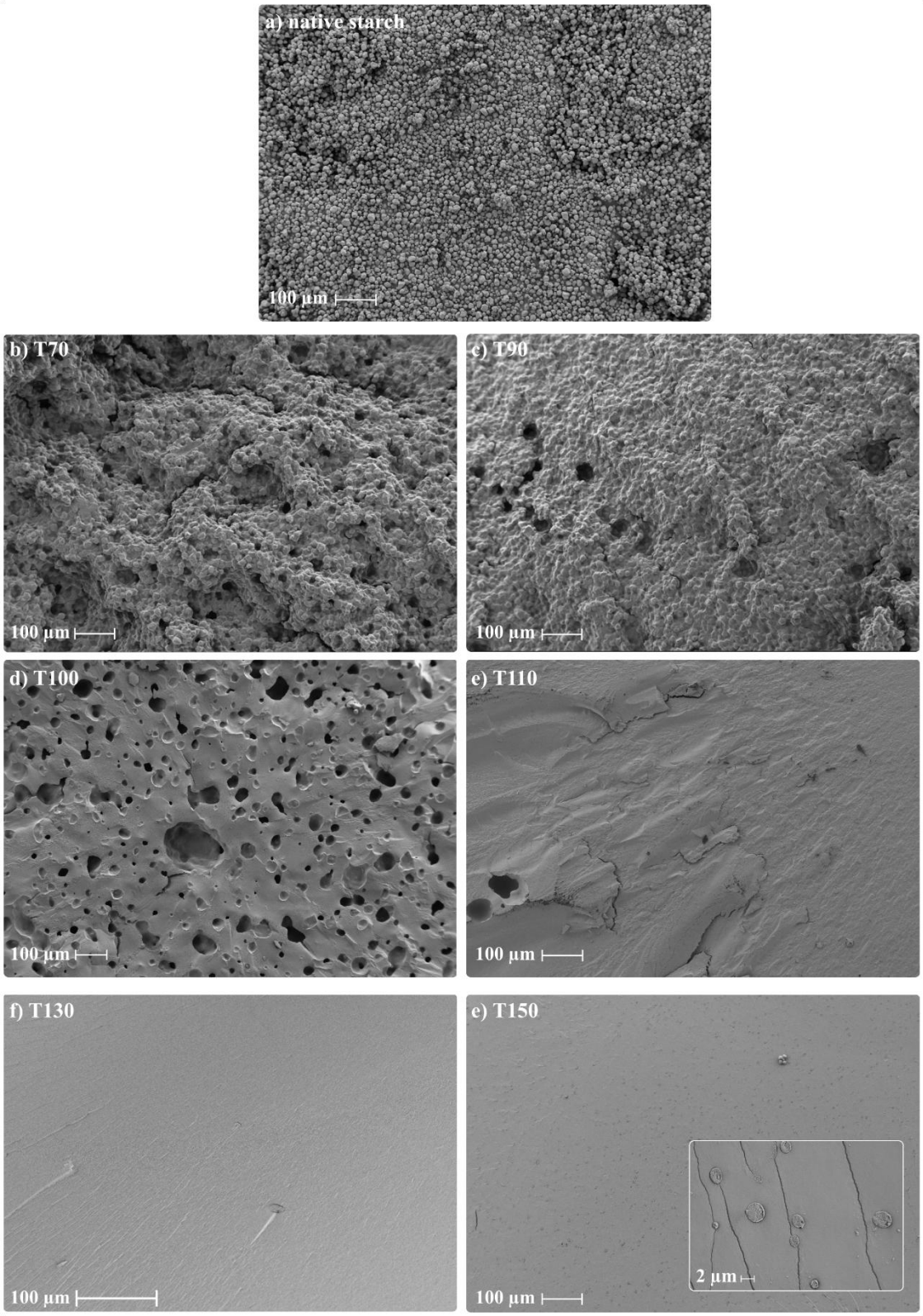

Fig 3 a) Corn starch granules and TPS obtained at different processing temperature profiles: b) T70 °C, b) T90 °C, d) T100 °C, e) T110 °C, f) T130 °C and g) T150 °C

The X-ray diffraction (XRD) patterns obtained for all thermoplastic starch materials prepared at different temperature profiles are presented in Fig 4 with native corn starch XRD pattern for comparison. Native corn starch XRD pattern shows a type A crystallinity typical of cereals, characterized by a strong intensity peak at 2θ = 15.2°, a double peak at 2θ =17.2° and 18.1°, and another strong intensity peak at 2θ = 23° (Angellier et al., 2006). After the extrusion process, the crystalline structures of native starch change with all the temperature profiles since the shape of all peaks changes from an A-type crystallinity to a V-type crystallinity, and the halo of the curve is modified. The crystallinity of the samples significantly decreases concerning native corn starch due to the granular disruption of starch due to the extrusion process (Angellier et al., 2006; Castillo et al., 2019). The V-type crystallinity in TPS, in which natural crystals have been mainly destroyed by the combination of temperature and shear forces, is produced because starch chains compounded with glycerol and water can crystallize during hot-melt extrusion (Chen et al., 2020). Moreover, the diffractograms show that the crystalline peaks and the amorphous halo of thermoplastic starch are dependent on the processing temperature. T70 presents similar peaks to those of native starch, at 2θ =15°, a double peak at 2θ = 17° and 18°, a peak at 2θ = 23°, as well as a new low-intensity peak centered at 2θ = 19.7° associated to crystallinity induced during processing (V_H-subtype) (Chen et al., 2020). In the XRD of T90, low-intensity peaks of V_H- subtype crystal structure (12.6°, 19.6°, and 22.4°) formed by the crystallization of amylose during hot-melt extrusion or during cooling are observed. However, residual A-type crystallinity peaks are still seen at 15° and 17.2° due to non-plasticized starch. Therefore, temperature profiles of 70 °C and 90 °C are not enough to completely disrupt native corn starch granules, confirming the FESEM characterization results. T100, T110, and T130 display V_H-type peaks at 2θ = 12.6°, 19°, and 22° and present the typical amorphous halo of semicrystalline thermoplastic starches centered on 19° (Campos et al., 2013a; Ostafińska et al., 2017). Besides, the absence of A-type crystal peaks confirms that the starch structure was completely destructured in these TPSs (Mendes et al., 2016). The intensity in the V_H-type peak centered at 19.7º could be related to the progress in the formation of thermoplastic starch. T70 and T90 present a low-intensity peak, which indicates incomplete plasticization. T100 and T110 present a medium-intensity peak, indicating that the material is plasticizing to form TPS. T130 displays a high-intensity peak, showing further plasticization and formation of the TPS structure. Finally, T150 presents a shift of the peaks to 18º and 21º, pointing to a transition to an A-type structure due to retrogradation (Lendvai et al., 2019). Besides, the XRD pattern of T150 significantly reduces the amorphous fraction of TPS since the amorphous halo is almost flat, which shows that this material is more crystalline than those obtained at lower temperatures. This behavior agrees with the FESEM observations, where the material's recrystallization was inferred due to the thermomechanical degradation in the extrusion process. Moreover, T100, T110, and T130 XRD patterns have a peak at 16.8°, which is associated with the recrystallization of short chains of amylopectin produced by short-term aging (B-type crystallinity) (Campos et al., 2013b).

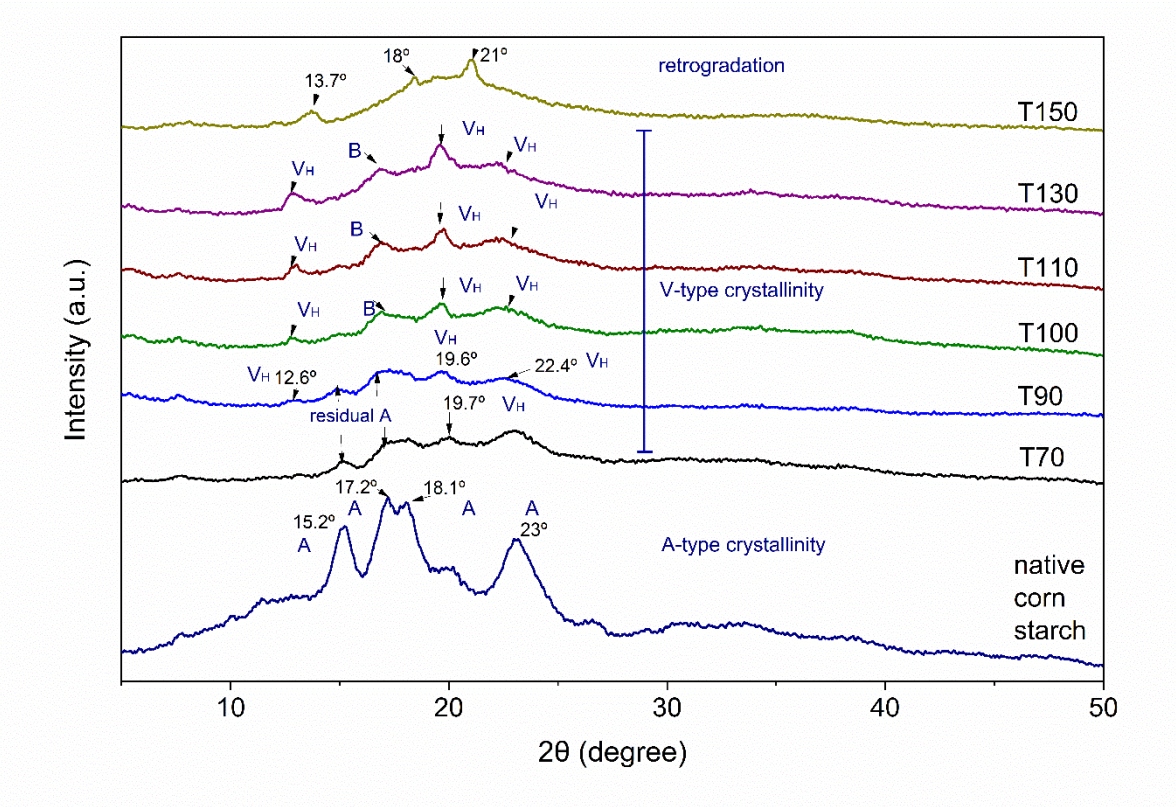

Fig 4 X-ray diffraction patterns of native corn starch and thermoplastic starch (TPS) processed at different temperature profiles T70, T90, T100, T110, T130, and T150

Fig 5 plots the FTIR spectra of thermoplastic starches processed at different temperatures. Changes in the spectra are found in the O-H stretching and -C-H stretching groups Fig 5-b. The O-H stretching, typically located at around 3300 cm^{-1} in TPS-based materials (Romeira et al., 2021), is located at 3283 cm^{-1} in T70, at 3325 cm^{-1} in T90 and T100, at 3338 cm^{-1} in T110 and T130, and 3340 cm^{-1} in T150. As Zong et al. stated, this hydroxyl group's vibration shift to higher frequencies from T70 to T150 results from the temperature increase, which causes the hydrogen-bond interaction to break down. (Zhong et al., 2022) Moreover, the –CH stretching band's intensity at 2928 cm^{-1} increases with temperature. The growth in the intensity –CH band accompanied by the shift of –OH wavenumber with increasing temperature can suggest that the hydrogen bond between starch becomes weaker as new bonds are formed due to the plasticization. The –OH peak's intensity increases when temperature increases from 100ºC to 130 ºC. This behavior shows that the rise in temperature to higher values than 100ºC (i.e., T110 and T130) enhances the interaction between the plasticizer and the hydroxyl groups, allowing –OH groups from glycerol to destroy the original hydrogen bonding interactions between starch molecules, which in turn make it thermoplastic (Shi et al., 2007). In T150, the peak intensity decreases, accompanied by the peak shift to a higher frequency, suggesting a decrease of the average strength of the hydrogen bonds and a broadening of the distribution (Dang & Yoksan, 2015). Regarding the fingerprint region of the spectrum, three characteristic peaks appeared between 1200 and 900 cm^{-1}, ascribed to the C–O bond stretching of starch: at 1150 cm^{-1}, there is a peak attributed to the C–O bond stretching of the C–O–H group in starch. Two additional peaks at 1080 and 1020 cm-1 arescribed to the C–O bond stretching of the C–O–C group in the anhydroglucose ring (X. Ma et al., 2007). X. Ma et al. (2007) studied starch plasticized with different plasticizers and attributed

the shifts of the C-O bond stretching peaks to the interaction between starch and plasticizers (X. Ma et al., 2007). According to Pawlak and Mucha (2003), the lower the peak frequency, the stronger the interaction (Pawlak & Mucha, 2003). Fig 5-c shows that T110, T130, and T150 interact more with the plasticizer than T70, T90, and T100. The three TPS samples have a higher wavenumber (lower frequency) than 1120 cm^{-1}. Nevertheless, T130 presents the highest wavenumber (1125 cm^{-1}), indicating the best interaction between starchy polymeric matrix and glycerol.

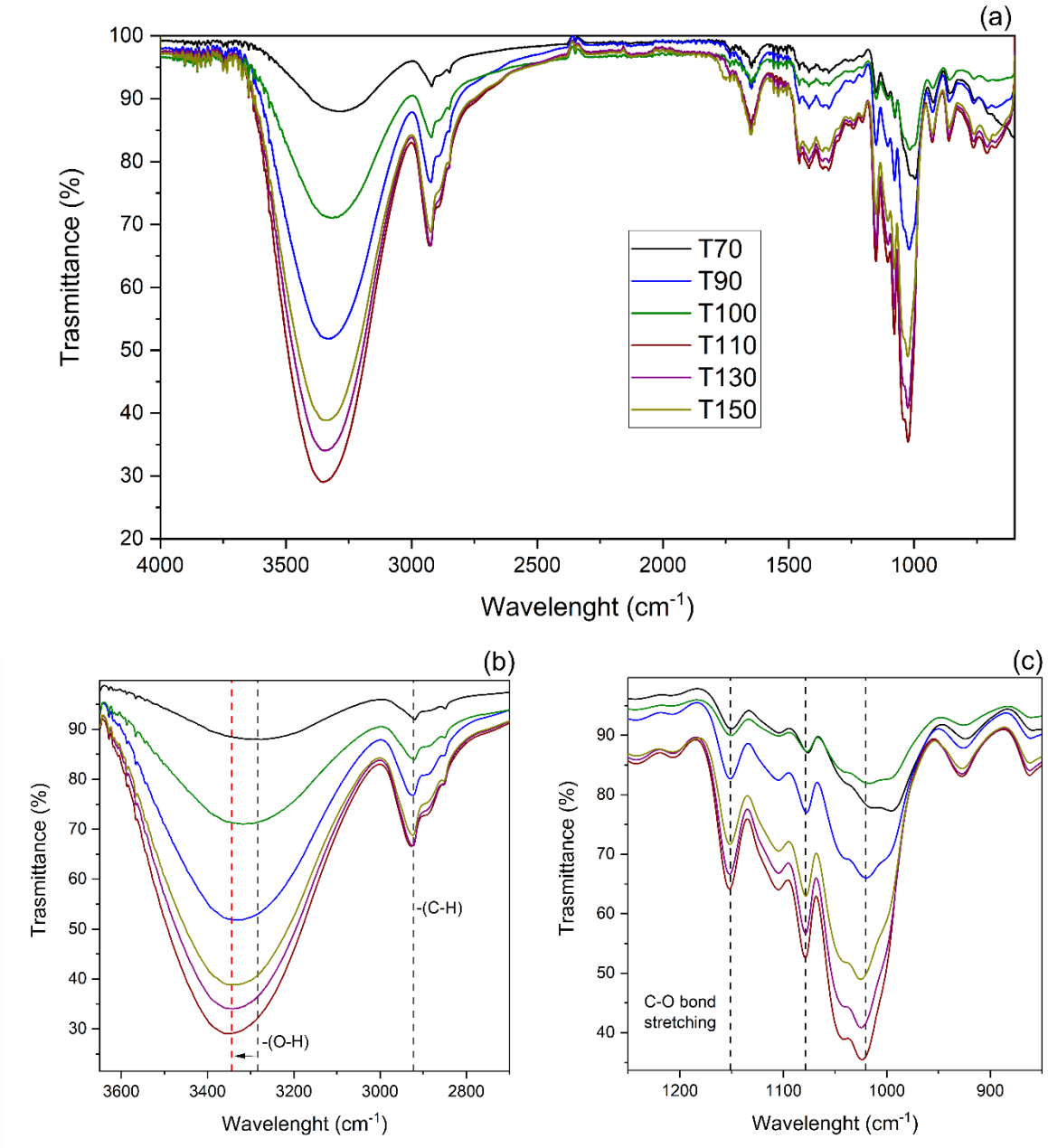

Fig 5 (a) FTIR spectra of thermoplastic starch (TPS) processed at different temperature profiles T70, T90, T100, T110, T130, and T150 (b) expanded area of -O-H stretching and -C-H stretching groups and (c) expanded area of C-O bond stretching

2.3. Mechanical characterization

The material's mechanical resistance is of fundamental importance in food packaging because it is required to protect the food from its surroundings during transport and storage. Table 3 shows the mechanical properties obtained from the tensile strength test. Fig 6 displays the typical stress-strain curve for the different studied starchy materials. Regarding Young's modulus, materials T70, T90, and T150 present a modulus of up to six times greater than T100, T110, and T130. In T70 and T90, this stiffening effect is produced by the unplasticized starch granules in the TPS polymeric matrix, as verified through FESEM micrographs (Fig 3-a and Fig 3-b). These starch granules could act as fillers, thus reinforcing the polymeric matrix. Sessini et al. (2016) studied TPS reinforced with starch nanoparticles. The starch-based nanofillers reinforce the TPS matrix due to the nanoparticles and matrix interaction (Sessini et al., 2016). In the present work, the good interaction between unplasticized starch granules and the TPS polymeric matrix increases the elastic modulus value. However, the granules also constitute stress concentration points (physical joints) in T70 and T90 materials, which also produce a decrease in the flexibility and the resistance of thermoplastic starch, as can be seen in the tensile strength and elongation at break values (Table 2) which resulted in the lowest when are compared to the materials processed at higher temperatures.

Table 3. Tensile properties of the TPS obtained at different temperatures.

Sample label	Young's modulus (MPa)	Tensile strength (MPa)	Elongation at break (%)	Toughness (kJ/m^3)
T70	12.6 ± 1.5^{a}	0.17 ± 0.11^{a}	4.5 ± 1.8^{a}	7 ± 3^{a}
T90	20.4 ± 1.9^{b}	0.42 ± 0.03^{b}	5.5 ± 0.4^{a}	12 ± 1^{a}
T100	5.1 ± 0.3^{c}	0.45 ± 0.03^{b}	22.2 ± 2.1^{b}	60 ± 2^{b}
T110	4.4 ± 0.3^{c}	0.95 ± 0.11^{c}	34.4 ± 6.3^{c}	304 ± 14^{c}
T130	5.2 ± 0.7^{c}	0.82 ± 0.06^{c}	70.1 ± 4.3^{d}	380 ± 53^{d}
T150	32.2 ± 2.7^{d}	3.28 ± 0.20^{d}	169.5 ± 30.1^{e}	4832 ± 535^{e}

[a-d] Different letters within the same property show statistically significant differences between formulations ($p < 0.05$)

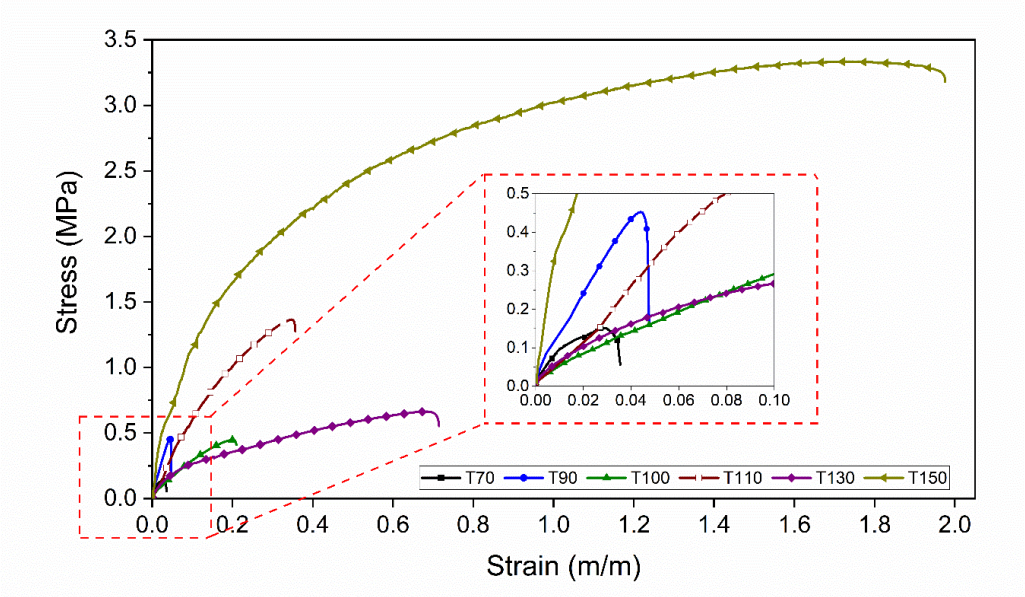

Fig 6 Typical stress-strain curve of filaments of TPS obtained at different processing temperature profiles

T100 displayed a low Young's modulus and tensile strength, attributed to the porosities observed in the microstructural characterization of this material, caused by the water evaporation from the blend when the material was extruded, as was verified in the FESEM analysis (Fig 3-d). These pores act as stress concentrators, which lead to a material with low tensile strength and, in general, poor overall mechanical performance (Mitrus, 2009). However, the significant increase in the elongation at break in T100 concerning T70 and T90 indicates that the material has begun to plasticize. T110 and T130 also present a progressive intensification in the elongation at break values, indicating greater plasticization. The elongation at break of T130 is statistically greater ($p < 0.05$) than the elongation at break of T100 and T110, indicating greater cohesion of the structure and, therefore, higher plasticization. Moreover, no significant differences ($p > 0.05$) were found for Young's T100, T110, and T130 modulus. Tensile strength significantly increases in T110 and T130 to T100, indicating better cohesion due to the absence of holes and higher cohesion.

The mechanical properties of starchy materials are dependent on the interaction between the polymeric matrix and the additives used, achieving a good plasticization effect when good flexibility, low brittleness, as well as improved stretching ability, are obtained (Arredondo Ochoa et al., 2017). The similarity in the mechanical properties values (Table 2) and the changes in the microstructure seen in the FESEM micrographs (Fig 3) indicate that the materials begin to plasticize at temperatures of 100 °C. These processing conditions allow the breakage of starch granules by the shear action due to the extrusion process and the temperature, which disrupts the starch granules, producing a greater interaction with the plasticizer and allowing a better plasticization (Paridah et al., 2016; Van Soest et al., 1996).

T150 seems to have the best mechanical properties among all the studied samples, showing much higher modulus values, tensile strength, and elongation at break. FESEM micrographs (Fig 3) of T150 exhibit crystalline domains, which increase the mechanical properties of the starchy material. Conversely, as the material suffers thermal degradation during the extrusion process at high temperatures, the resultant material is a highly plasticized starch with crystalline structures inside. Moreover, within T150, shorter starchy polymeric chains are generated because of the polymer thermal degradation. These chains contribute to the maximum elongation at break of these materials. On the other hand, crystalline structures act as reinforcing elements, according to Mathew and Dufresne. (2002), there is also a crosslinking effect (between the amorphous and crystalline parts) that improves the material mechanical properties (Mathew & Dufresne, 2002). Consequently, when T150 experiments with a tensile deformation, the crystalline domains, and polymer chains are reoriented toward the applied stress, and strain hardening occurs. As a result, the material toughness increases (Paiva et al., 2018). Table 3 displays the toughness values of the materials T150 has the highest toughness due to the strain hardening. Moreover, T130 has a higher toughness than T110, indicating a higher plasticization for T130. Meanwhile, T70 and T90 reported the lowest toughness value due to plasticization failures.

Fig 6 shows an average stress-strain curve of the studied blends. In the graphic, T110 and T130 present close toughness. However, T130 has higher elongation, which is typical for a plasticized material. T100 also has a characteristic stress-strain curve of a plasticized material. However, the presence of porosities in the material detracts from the properties of the TPS. Finally, T150 also showed the typical stress-strain curve of plasticized starch. At temperatures greater than 100 °C, under the processing conditions described in this study, starch can be plasticized, presenting partial plasticization at T100 and T110 and high plasticization at T130 and T150. Even when T150 presents good overall tensile properties, it shows signs of thermal degradation, which is essential for future applications due to the color characteristics and, most importantly, because the material already exhibits signs of retrogradation.

2.4. Thermal characterization

Fig 7 compares the thermal decomposition curves of TPS processed at different temperatures and pure starch. For all the analyzed materials, the thermal degradation curve (TGA) presents three decomposition stages (Fig 7-a). In the case of pure starch, according to Paridah et al. (2016), the first stage occurs up to 120 °C and matches the loss of free water in the starch (Paridah et al., 2016). In the starch curve (solid blue line), the curve remains constant without mass loss between 160 °C and 290 °C after an initial mass loss. For plasticized materials at different temperatures (TPS), the limits of the decomposition stages are found at higher temperatures than those of pure starch. The first stage, for instance, extends until temperatures of 290 °C. At this stage, the degradation occurs in two steps. Yunos and Rahman (2011) attribute this phenomenon to the effect of glycerol on starch-based polymers (Yunos & Rahman, 2011). For all processed TPS, the material loss due to evaporation of free water in the material occurs between 35 °C and 160 °C. In comparison, between 160 °C and 290 °C, it is considered that happens the loss of the bound water of the material (Ismail et al., 2017; Paridah et al., 2016) together with the evaporation of the glycerol that starts at 200 °C and ends around 300 ° C (Shi et al., 2007; Yunos & Rahman, 2011). In this way, in the first stage of thermal decomposition, the plasticizers (water and glycerol) are removed from the TPS structure during TGA heating.

In the second stage of thermal degradation, which takes place from 290 °C to 336 °C, the breakage of the starch chains and the oxidation of the glucose rings occurs (Ismail et al., 2017). During the second stage, TPS showed lower thermal stability than neat starch. This behavior has been ascribed to the ability of glycerol to reduce the inter-and intra-molecular bond interaction within the starchy polymeric matrix, which decreases the material's thermal stability (Sessini et al., 2016). Finally, in the third thermal decomposition stage, organic waste is degraded and the residue is turned into ashes (Paridah et al., 2016).

The second and third stages of thermal decomposition are similar to all the studied TPS, with slight variations in the shape of the curve and the temperature ranges linked to the processing temperature profiles. Finally, in Fig 7-a, there is a very marked difference between the TPS studied and the pure starch due to the action of the plasticizer on the amylose and amylopectin chains, which gives it greater thermal resistance. In this way, the shape of the TGA curve corroborates that all the TPS formulations were plasticized to some degree despite the processing temperature. The formed materials can be classified into three groups if compared to starch: highly plasticized starch (T130 and T150), partially plasticized starch (T100 and T110), and incompletely plasticized (just a mixture of plasticizers and starch granules) (T70 and T90).

In the case of T130 and T150, in the first stage, the mass loss of these blends is less pronounced than that of the other materials analyzed. To extend this observation, Table 4 reports the values for the onset decomposition temperature ($T_{5\%}$), the end decomposition temperature ($T_{90\%}$), and the temperature of the maximum decomposition rate (T_{max}).

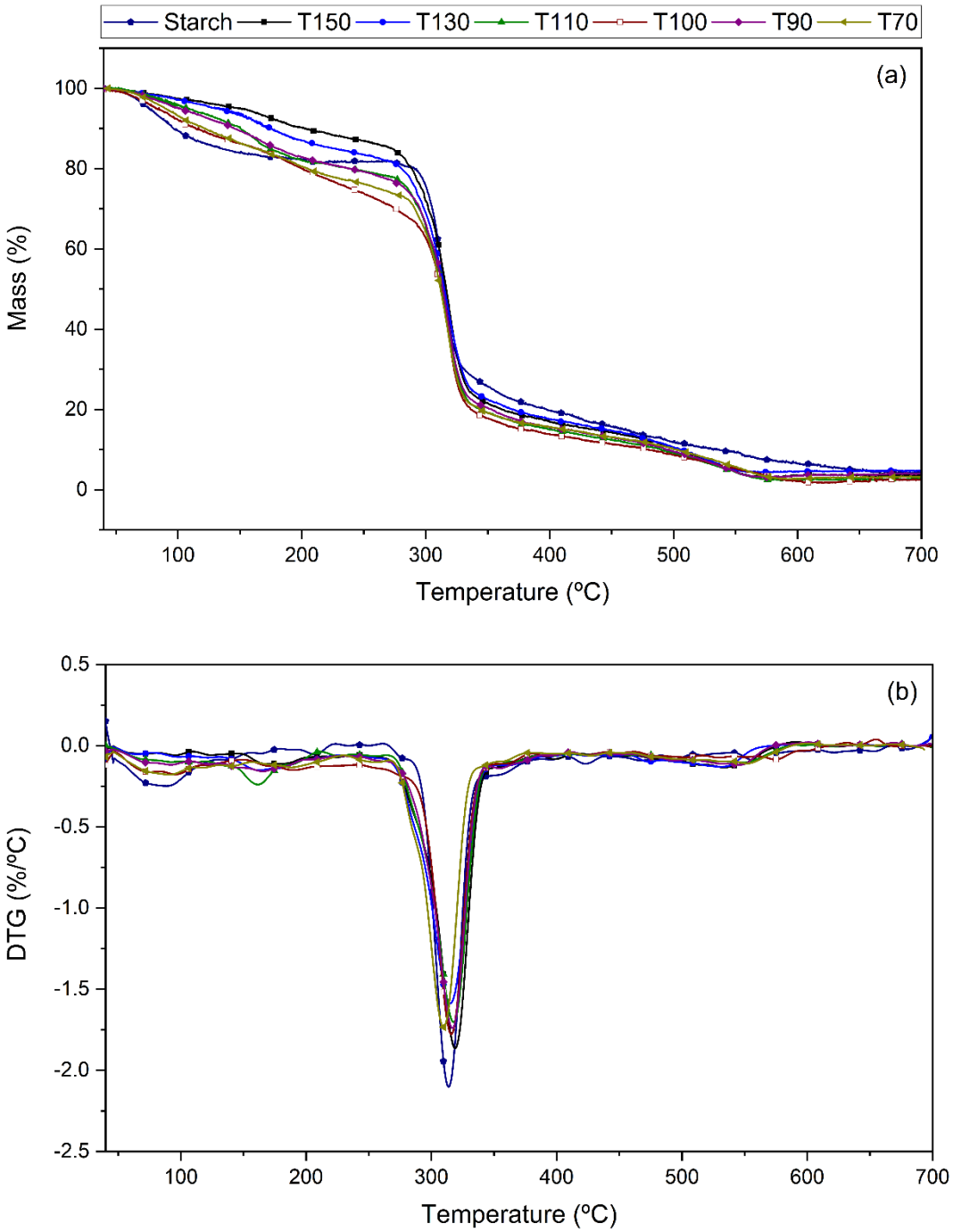

Fig 7 a) TGA and b) DTG curves of neat starch and obtained TPS at different extrusion temperature profiles

Table 4. Onset decomposition temperature ($T_{5\%}$), Temperature of maximum decomposition rate (T_{max}), and end decomposition temperature ($T_{90\%}$) for neat starch and the TPS obtained at different extrusion temperature profiles.

Sample label	$T_{5\%}$ (°C)	T_{max} (°C)	$T_{90\%}$ (°C)
Starch	76.6	314,5	532,7
T70	89.5	316.0	501.9
T90	100.7	317.1	494.6
T100	82.5	317.9	479.1
T110	107.7	319.6	489.6
T130	130.1	316.7	505.6
T150	150.5	317.6	504.2

In Table 4, based on the $T_{5\%}$ values, it is noted that the material's thermal stability increases with the increase in the extrusion temperature profile. An exception to this trend is the material processed at 100 °C (T100), in which the onset decomposition temperature is lower than the other studied formulations. The water evaporation at the outlet of the extruder machine can explain this. The material becomes less thermally stable because the water reaches its boiling point and evaporates quickly from the polymeric matrix, thus generating a greater free volume and porosity. In addition, there is less chance that water will completely gelatinize the starch matrix, making the material more susceptible to thermal degradation (Mitrus, 2009).

The increase in thermal stability confirms the TPS plasticization process. As discussed before, if the processing temperature profile increases, the granule breakage improves, so the number of starch granules that plasticize during the process increases. In this way, the starch chains interact, so high temperatures will be required to degrade the material structure, resulting in a higher thermal resistance (Nafchi et al., 2013; Paridah et al., 2016). For T150, $T_{5\%}$ is around 15% and 60% higher than T130 and T70, respectively, ascribed to the recrystallized structures in the material previously observed in FESEM images (Fig 3-g). These structures confer higher thermal stability since they require a higher temperature to degrade themselves, thus delaying the start of thermoplastic starch thermal decomposition. When the chain decomposition process begins in the second and third stages, there are no significant changes in T_{max} or $T_{90\%}$ for plasticized materials (TPS) because, after the plasticizers' evaporation (water and glycerol, from 290 °C), the composition of the materials is the same in all cases. However, for neat starch, the thermal stability is greater in these stages due to the granules not being subjected to disruption processes (extrusion and temperature), so it requires a higher temperature for its complete degradation, as shown in the $T_{90\%}$ value (Table 4.

Fig 8 shows the differential scanning calorimetric curves obtained from the first and second DSC heating scans for the different TPS obtained at different processing temperatures. This technique cannot detect the glass transition temperature of TPS as no inflection point is observed in the obtained DSC curves. The TPS thermal transitions reported in the literature for starch-glycerol materials (Aldas, Pavon, et al., 2020a; Rodriguez-Gonzalez et al., 2004; Wattanakornsiri et al., 2012) are not readily observable by this technique. According to Averous and Boquillon (2004) and Averous et al. (2001), at the glass transition temperature, TPS presents a low drop in heat capacity, so it is sometimes challenging to detect the glass transition of this material using analysis (Avérous et al., 2001; Averous & Boquillon, 2004). For the temperature range analyzed (-50 to 170 °C), the literature indicates that there is a thermal transition ascribed to the starch-rich phase (α relaxation), whose transition temperature (Tα) is between 34 and 70 °C and that it varies depending on the glycerol content and the moisture amount present in the material (Forssell et al., 2002; Wang & Huang, 2007b; Wattanakornsiri et al., 2012).

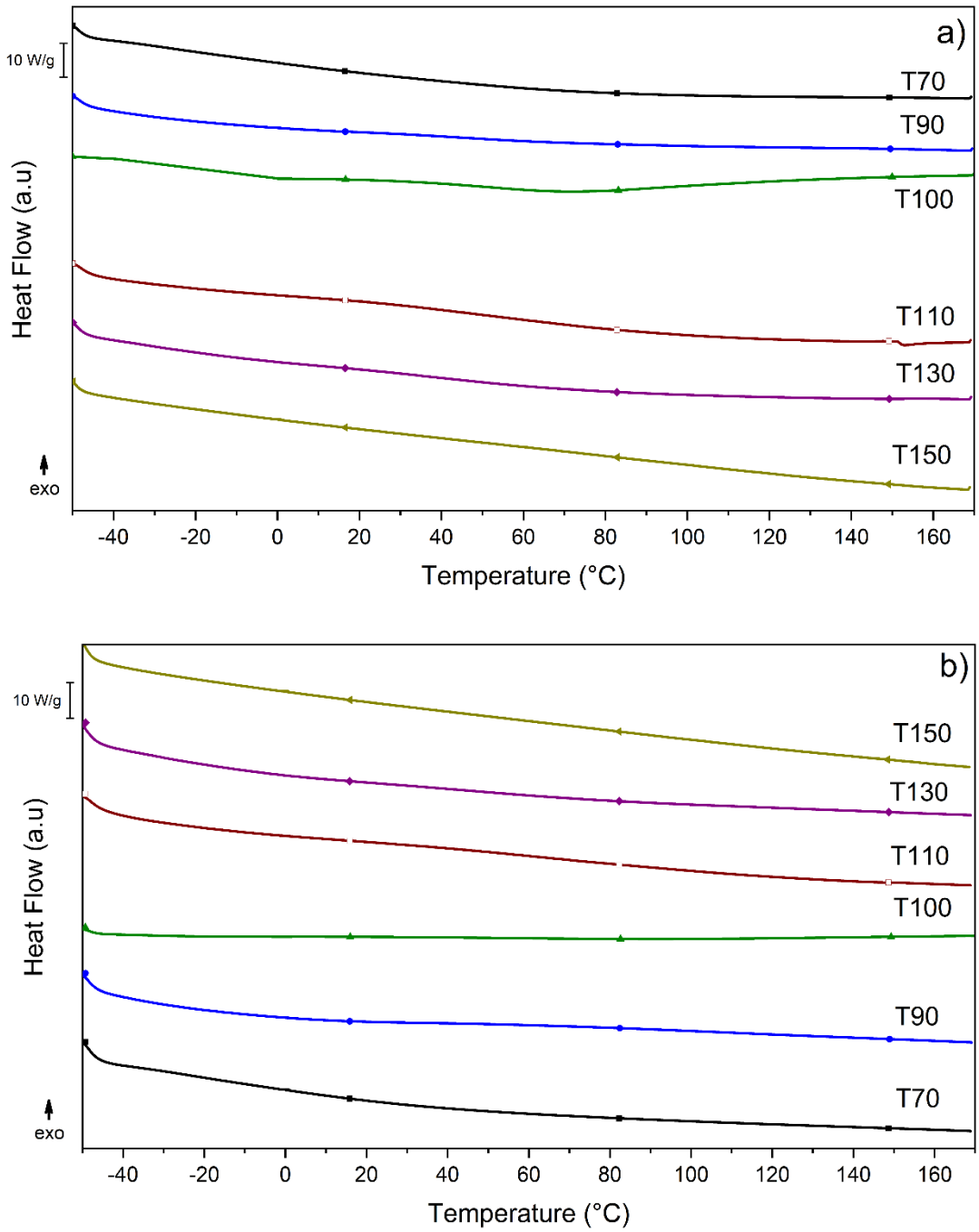

Fig 8 DSC a) first and b) second heating curves for TPS obtained at different extrusion temperature profiles

The DTMA is a technique that detects thermal transitions more accurately (Averous & Boquillon, 2004). Fig 9 shows the variations of the loss factor (tan(δ)) and the storage modulus (G') with temperature for all the studied materials. The tan (δ) curves (Fig 9-a) showed a heterogeneous system

with two relaxations (peaks), between -60 °C and -40 °C and between 20 °C and 40 °C. The heterogeneity of the studied TPS is due to a phase separation with glycerol-rich domains (β relaxation) and starch-rich domains (α relaxation) (Enrione et al., 2010; Taguet et al., 2009). Therefore, each peak is so-called T_β and T_α, respectively, being T_β a secondary transition of TPS and T_α a primary transition of TPS (Taguet et al., 2009; Teixeira et al., 2012).

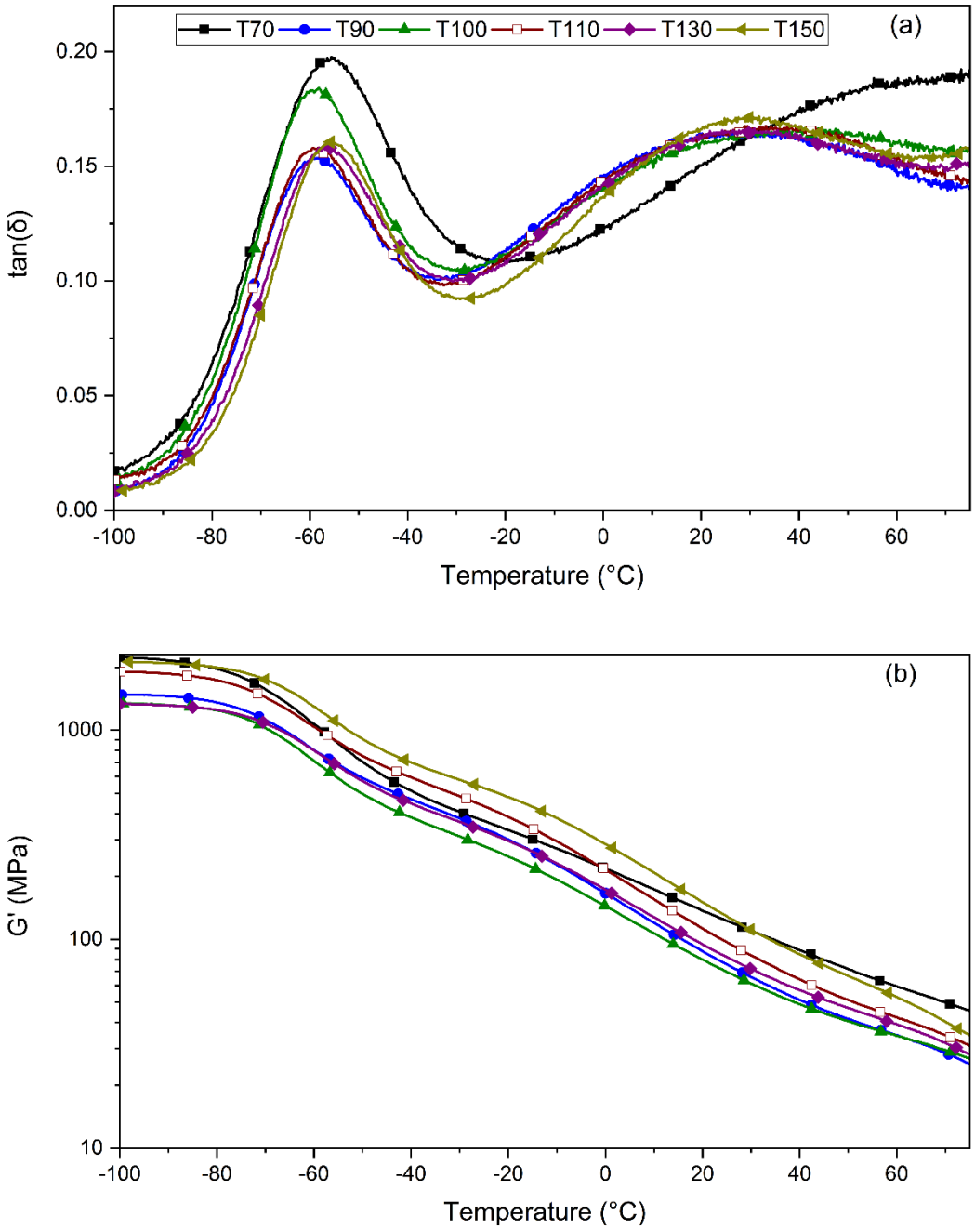

Fig 9 a) loss factor and b) storage modulus obtained from DMTA analysis for TPS containing 25 % glycerol and 10 % water processed at different temperature profiles

No differences were found in T_β (located at ~ -57 °C) and T_α (located at ~ 30 °C) of T90, T100, T110, T130, and T150. Notably, T70 shows a broader and poor unresolved T_α peak, and its T_β endset temperature is 10 °C higher than other TPS systems. This behavior confirms that starch was not completely plasticized at the temperature profile of 70 °C. Additionally, at higher processing temperatures than 90 °C, the extrusion temperature profile has a negligible effect on the TPS thermal transitions (T_α and T_β). The breadth of the T_α transition peak of Fig 9-a of all the studied TPS is in good accordance with the literature (Averous & Boquillon, 2004; Wattanakornsiri et al., 2012). The broadness of the peaks points to a strong polydispersity in TPS due to different polymer chain lengths. Therefore, this explains the vague resolution of the thermal transitions in the DSC assessment and shows that this transition could only be observed with a DMTA analysis (Foreman, 2008).

Regarding the storage modulus (G') plotted in Fig 9-b, the two identified relaxations, β and α relaxations, have two corresponding falls in the G' of the materials, at -63 °C and 25 °C, respectively. These falls show a reduced TPS stiffness (Chartoff & Sircar, 2005). The G' curves show that from -100 °C to 25 °C, T150 has the highest storage modulus among the studied formulations. In temperatures above 30 °C, the G' of the T150 formulation constantly drops to similar values of the other formulations because the T_α was reached. Moreover, the storage modulus curve shows that T70 material does not lose G' as fast as the other formulations because the plasticization was incomplete, and, consequently, the material does not have a thermoplastic behavior. As already discussed, the results confirm the good plasticization effect obtained for the extruded materials at temperatures above 100 °C.

At 25 °C, T150 displays the highest storage modulus (117 MPa), followed by T110 (93 MPa) and T130 (80 MPa). However, the differences between the storage modulus of T110 and T130 are not too marked, as the tensile test results T110 and T130 statistically have the same Young's modulus. At the same time, T150 displays a higher value and suggests a similar outcome in the storage modulus. T100 material presents a lower storage modulus (68 MPa) than T110, T130, and T150 due to its limited structure resistance because of the formed holes. T70 and T90 are not wholly plasticized materials; therefore, their storage modulus cannot be compared with Young's modulus. These results agree with the DRX patterns, an incomplete plasticization for T70 and T90 and a plasticized material for T100, T110, and T130.

2.5. Water contact angle

Water resistance is critical in materials intended for food contact applications (He et al., 2020). Surface wettability was conducted to study the hydrophilic/hydrophobic behavior of the film surfaces by determining the water contact angle. Fig 10 displays the WCA comparison between the different TPS. The TPS-based materials mainly showed hydrophilic surfaces, as films from T70 to T130 presented smaller water contact angle values than 65° (Hambleton et al., 2009), in good accordance with previous results (Pavon et al., 2021). The hydrophilic surface of TPS-based materials is due to the high number of hydroxyl groups in starch molecules (He et al., 2020). In addition, the WCA of TPS decreased with the plasticizer as it increased the polymer chain mobility (Dang & Yoksan, 2021). The lowest values were observed for T70 and T90 (WCA_{T70}= 55.3 ± 1.7º and WCA_{T90}= 53.6 ± 0.2º). This result could indicate more free OH groups in these formulations. T100 shows a slight increase in the WCA (WCA_{T100}= 57.4 ± 0.4º). This behavior can be related to the fact that this material has less water to interact with at the surface, as at this processing temperature, the water evaporates just as the filament leaves the extruder. T110 and T130 showed an additional increase in the WCA values (WCA_{T110}= 64.4 ± 1.2º and WCA_{T130}= 63.2 ± 0.8º), which could be related to the fact that these processing temperatures permitted the disruption of the starch granules, leading to less –OH groups exposed to the surface. Finally, T150 showed the highest WCA value of WCA_{T150}= 67.1 ± 0.7º). The

wettability is strongly dependent on the surface chemical and topographical properties; therefore, in T150, due to the recrystallization process, crystalline structures appear, thus affecting the roughness of the film and somewhat increasing the hydrophobicity of the surface.

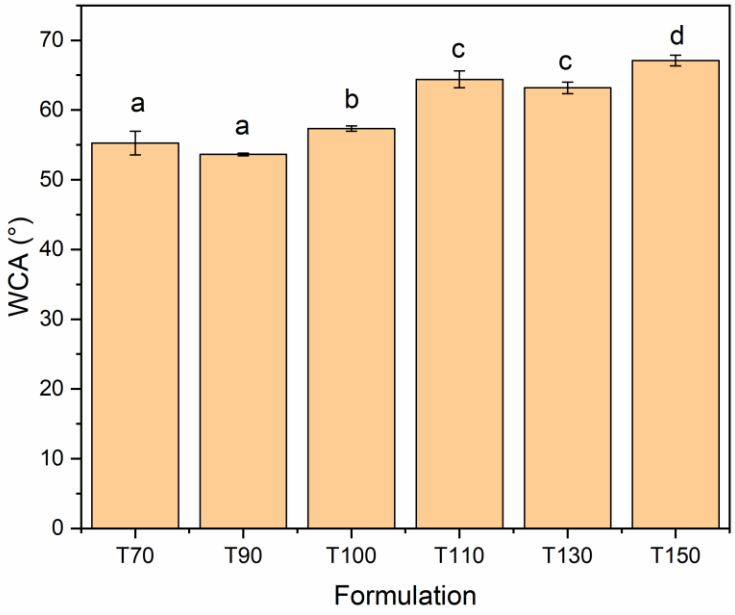

Fig 10 Water contact angle measurements of the TPS obatained at different temperatures. [a-d] Different letters within the same property show statistically significant differences between formulations ($p < 0.05$)

2.6. Water Uptake

Water absorption represents one of the most essential characteristics of TPS-based products for many food contact applications, i.e., packaging, compostable agricultural films, and bags. The strong hydrogen bonds of starch hold the starchy polymeric chains together when submerged in water, making starch granules not soluble in cold water. Nevertheless, partial solubilization of starch occurs since the crystalline structure is disrupted in the TPS-obtaining process. Thus, water molecules can interact with the hydroxyl groups of amylose and amylopectin (Jiménez et al., 2012), and this is directly related to the water uptake of the TPS-based materials. Fig 11 presents the different TPS water absorption curves. All the studied materials show a swift initial water absorption within the first 15 minutes of the test. Hoffman (2012) attributed this behavior to the hydrophilic nature of the starch and glycerol materials. In this way, the water that enters the material during the water uptake test interacts with the hydrophilic groups of thermoplastic starch, producing hydration of the system (Hoffman, 2012). After 15 minutes of testing, the behavior of the studied materials can be divided into three groups. First, the materials T90 and T70, with the lowest WCA and higher surface hydrophilicity, presented a maximum water absorption of 37% at 15 and 30 minutes of testing, respectively. Both materials suffered ruptures of the test specimens due to swelling by water absorption. Then, T110 and T130 reached the water absorption equilibrium at 60% after 360 minutes (6 hours) of testing. These two formulations did not suffer breaks by swelling during the test. The third group is T100 and T150, which also failed (break by swelling) at 64 minutes with a water absorption percentage of 78% and 180 minutes with a water absorption percentage of 86%, respectively. The failures detected during the T70, T90, T100, and T150 tests occurred since, after fast hydration of the TPS during the first 15 minutes, the water continues to enter the material and occupies the existing free volume between the chains. When the free volume is complete, the chains reach a limit where they can no longer expand and, in turn, produce a general swelling of the material.

However, because of the osmotic force of the chains, the water continues to enter within the material's structure. It exceeds the existing free volume, which produces an over-swelling of the material structure and the consequent collapse of the system with a failure due to hydration (Hoffman, 2012; Neus Angles & Dufresne, 2000).

The diverse behavior of the materials detected for this test corroborates the influence of the extrusion temperature profile on the TPS plasticization process. On the one hand, the materials T70 and T90 suffer premature failure due to the incomplete plasticization process of the material's structure during the water absorption. In the case of the T100 and T150 materials, with partially or fully plasticized structures, as observed by FESEM (Fig 3-d and Fig 3-g), the initial water absorption is higher than in the other TPS, reaching around 80%. In T100 material, the structure presents porosities that facilitate water penetration and increase the free volume in the material, and it allows the fast entry of a greater quantity of water (Hoffman, 2012; Neus Angles & Dufresne, 2000). Nevertheless, these same holes decrease the swelling resistance, so the material structure collapses after 64 minutes of testing. In contrast, T150 absorbed up to 86% of its weight since it presented a high elongation at break (as shown in the values in Table 4), allowing greater diffusion of water within its structure before breaking (Sen et al., 1998).

The break by swelling of the material can be linked to the reduction in the mobility of the amylopectin chains in this TPS, which produce rigidity of the swollen material due to the formation of crystalline structures, previously discussed (see red arrows in Fig 3-g) (Neus Angles & Dufresne, 2000). T110 and T130 have lower water absorption than T150 since they have a lower free volume. At the same time, they are the only TPS formulations that reach the steady absorption state without failure because of the flexibility of the material's chains, which can recover their shape after maximum swelling (Chang et al., 2010). These results corroborate the incomplete plasticization of T70 and T90 structures, while T100, T110, T130, and T150 present plasticized structures, which agrees with the results of the previous properties.

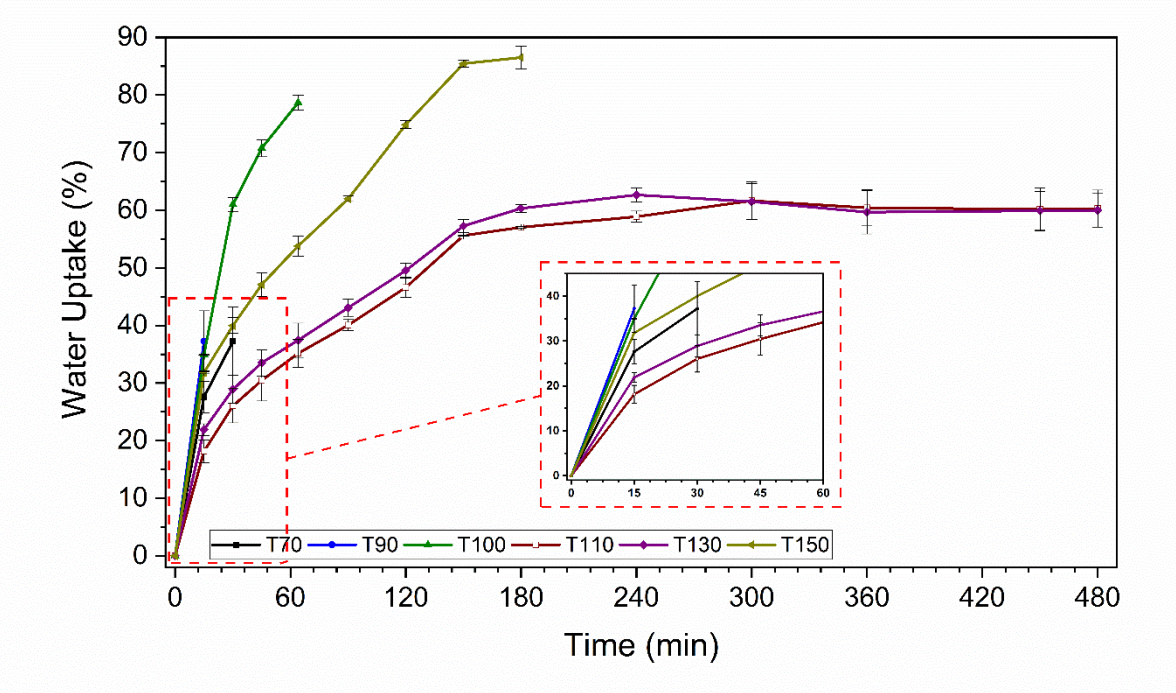

Fig 11 Water Uptake of TPS processed at different extrusion temperatures profiles.

3. CONCLUSIONS

This work studied the effect of the extrusion temperature profile on the plasticization of native corn starch using water and glycerol as plasticizers to obtain fully biobased and biodegradable thermoplastic starch by melt-extrusion simulating the industrial conditions for single-use plastic and packaging applications. With this purpose, this paper evaluated the thermal, mechanical, optical, and microstructural characteristics of thermoplastic starch obtained at six different temperature profiles (T70, T90, T100, T110, T130, and T150) not only to find the best processing conditions for the obtention of food-grade TPS for scalable production at the industrial level but also to understand the effect of the processing temperature on TPS-based materials final performance. The study also determined TPS's surface wettability and water absorption to gain insight into surface water affinity because these materials are intended for food contact applications. FESEM analysis showed that to produce a complete disruption of the starch granule, temperatures of 110 ºC or higher are needed. Materials obtained at 70 ºC and 90 ºC present incomplete plasticization, and therefore, they display higher surface hydrophilicity and poor mechanical behavior; meanwhile, T100, T110, and T130 present plasticized structures. T100 presents porosity in its structure because water evaporation occurs at the extruder die, affecting its overall mechanical properties. T110 presents some residues of starch granules that point to a partial plasticization effect of the starchy structure.

Moreover, even though T130 and T110 have statistically equal tensile moduli and tensile resistance, T130 presents a greater elongation at break than T110, which suggests that T130 has a higher degree of plasticization due to the complete disruption of the starchy granule. T150 displays good mechanical properties, but the material suffers thermal degradation, as seen by its color change and the yellowish index. Moreover, T150 FESEM images showed recrystallization due to the high-temperature processing conditions. Thermogravimetric analysis showed higher thermal stability in the TPS prepared at higher temperature profiles. DMTA test showed that at 25 °C, the storage modulus of T150, T130, and T110 can correlate with Young's modulus. However, as T100 presents a lower storage modulus because of the holes in its structure and T70 and T90 are not completely plasticized, the storage modulus of these materials cannot be correlated with tensile modulus. It was determined that water uptake depends on the plasticization of the structure, as T70 and T90 are materials with low water absorption and are prone to premature rupture. Meanwhile, T100, T110, T130, and T150 present high water absorption levels because the structure of the materials was partially or highly plasticized.

When processed into films, the formulations with improved granule disruption (T100, T110, and T130) showed more transparency than those with inadequate plasticization (T70 and T90). Furthermore, because starch has high -OH groups, all the films displayed hydrophilic surfaces. The attained results conclude a direct relationship between the TPS extrusion temperature profile used and the TPS overall performance. Glycerol and water can produce the starchy polymeric matrix transition from a glassy state to a thermoplastic state at temperatures between 110 and 150 ºC by using the melt-extrusion process, which is already established in the plastic processing industry, and allowing to obtain materials with good overall mechanical, thermal and able to withstand water absorption without the material breaking due to its swelling capacity. Finally, the processing temperature conditions of starchy-based materials affect the final properties conferred by the plasticization of the thermoplastic starch structure. The study of different processing temperatures developed here opens the possibility of using these processing conditions at the food packaging industrial level. Besides, the materials showed high transparency and surface hydrophilicity, making the TPSs attractive for dry food product applications.

Author contributions

Miguel Aldas: Methodology**,** Investigation, Writing - Review & Editing; **Cristina Pavon:** Validation, Investigation, Formal analysis, Writing - Original Draft; **Harrison De La Rosa-Ramírez:** Methodology, Investigation, Visualization; **Juan López-Martínez:** Funding acquisition, Resources, Supervision; **Marina P. Arrieta:** Conceptualization, Funding acquisition, Writing - Review & editing, Project administration

Funding

This research is a part of the grant PID2020-116496RB-C22 and PID2021-123753NA-C32 funded by MCIN/AEI/10.13039/501100011033 and by ERDF "A way of making Europe" by the "European Union" and by "Research Consolidation" Project (grant CNS2022-136064) funded by MCIN/AEI/10.13039/501100011033 and by the "European Union NextGenerationEU/PRTR".

Acknowledgments

Cristina Pavon thanks Universitat Politècnica de València for his post-doctoral PAID-10-23 grant. Microscopy Services at UPV are also acknowledged for their help in collecting and analyzing images. The authors thank Funding for open access charge: CRUE-Universitat Politècnica de València.

STATEMENTS AND DECLARATIONS

Declaration of Competing Interest

The authors declare that they have no known competing financial interests or personal relationships that could have appeared to influence the work reported in this paper.

Data availability: The data presented in this study are available on request from the corresponding author

REFERENCES

Aldas, M., Ferri, J. M., Lopez-Martinez, J., Samper, M. D., & Arrieta, M. P. (2019). Effect of pine resin derivatives on the structural, thermal, and mechanical properties of Mater-Bi type bioplastic. *Journal of Applied Polymer Science*, *137*(4), 48236. https://doi.org/10.1002/app.48236

Aldas, M., Pavon, C., Ferri, J. M., Arrieta, M. P., & López-Martínez, J. (2021). Films Based on Mater-Bi® Compatibilized with Pine Resin Derivatives: Optical, Barrier, and Disintegration Properties. *Polymers*, *13*(9), 1506. https://doi.org/10.3390/polym13091506

Aldas, M., Pavon, C., López-Martínez, J., & Arrieta, M. P. (2020a). Pine resin derivatives as sustainable additives to improve the mechanical and thermal properties of injected moulded thermoplastic starch. *Applied Sciences (Switzerland)*, *10*(7). https://doi.org/10.3390/app10072561

Aldas, M., Pavon, C., López-Martínez, J., & Arrieta, M. P. P. (2020b). Pine resin derivatives as sustainable additives to improve the mechanical and thermal properties of injected moulded thermoplastic starch. *Applied Sciences*, *10*(7), 2561–2578. https://doi.org/10.3390/app10072561

1012 Aldas, M., Rayón, E., López-Martínez, J., & Arrieta, M. P. (2020). A Deeper Microscopic Study of
1013 the Interaction between Gum Rosin Derivatives and a Mater-Bi Type Bioplastic. *Polymers*,
1014 *12*(1), 226–243. https://doi.org/10.3390/POLYM12010226

1015 Angellier, H., Molina-Boisseau, S., Dole, P., & Dufresne, A. (2006). Thermoplastic Starch-Waxy
1016 Maize Starch Nanocrystals Nanocomposites. *Biomacromolecules*, *7*(2), 531–539.
1017 https://doi.org/10.1021/bm050797s

1018 Apriyanto, A., Compart, J., & Fettke, J. (2022). A review of starch, a unique biopolymer –
1019 Structure, metabolism and in planta modifications. *Plant Science*, *318*, 111223.
1020 https://doi.org/10.1016/J.PLANTSCI.2022.111223

1021 Arredondo Ochoa, T., García-Almendárez, B. E., Reyes, A. A., Pastrana, D. M. R., López, G. F. G.,
1022 Belloso, O. M., & González, C. R. (2017). Design and Characterization of Corn Starch Edible
1023 Films Including Beeswax and Natural Antimicrobials. *Food and Bioprocess Technology*,
1024 *10*(1), 103–114. https://doi.org/10.1007/S11947-016-1800-4/FIGURES/7

1025 Arrieta, M. P., Peltzer, M. A., Garrigós, M. D. C., & Jiménez, A. (2013). Structure and mechanical
1026 properties of sodium and calcium caseinate edible active films with carvacrol. *Journal of Food*
1027 *Engineering*, *114*(4), 486–494. https://doi.org/10.1016/J.JFOODENG.2012.09.002

1028 Arrieta, M. P., Samper, M. D., Aldas, M., & López, J. (2017). On the Use of PLA-PHB Blends for
1029 Sustainable Food Packaging Applications. *Materials*, *10*(9).
1030 https://doi.org/10.3390/ma10091008

1031 Artz, W. E., Warren, C., & Villota, R. (1990). Twin-Screw Extrusion Modification of a Corn Fiber
1032 and Corn Starch Extruded Blend. *Journal of Food Science*, *55*(3), 746–754.
1033 https://doi.org/10.1111/J.1365-2621.1990.TB05220.X

1034 Auras, R., Harte, B., & Selke, S. (2004). An overview of polylactides as packaging materials. In
1035 *Macromolecular Bioscience* (Vol. 4, Issue 9, pp. 835–864). John Wiley & Sons, Ltd.
1036 https://doi.org/10.1002/mabi.200400043

1037 Averous, L., & Boquillon, N. (2004). Biocomposites based on plasticized starch: Thermal and
1038 mechanical behaviours. *Carbohydrate Polymers*, *56*(2), 111–122.
1039 https://doi.org/10.1016/j.carbpol.2003.11.015

1040 Avérous, L., Fringant, C., & Moro, L. (2001). Plasticized starch-cellulose interactions in
1041 polysaccharide composites. *Polymer*, *42*(15), 6565–6572. https://doi.org/10.1016/S0032-
1042 3861(01)00125-2

1043 Bastioli, C. (1998). Properties and applications of mater-Bi starch-based materials. *Polymer*
1044 *Degradation and Stability*, *59*(1–3), 263–272. https://doi.org/10.1016/S0141-3910(97)00156-0

1045 Bertoft, E. (2017). Understanding starch structure: Recent progress. *Agronomy*, *7*(3).
1046 https://doi.org/10.3390/agronomy7030056

1047 Campos, A., Teodoro, K. B. R., Teixeira, E. M., Corrêa, A. C., Marconcini, J. M., Wood, D. F.,
1048 Williams, T. G., & Mattoso, L. H. C. (2013a). Properties of thermoplastic starch and
1049 TPS/polycaprolactone blend reinforced with sisal whiskers using extrusion processing.
1050 *Polymer Engineering and Science*, *53*(4), 800–808. https://doi.org/10.1002/pen.23324

Campos, A., Teodoro, K. B. R., Teixeira, E. M., Corrêa, A. C., Marconcini, J. M., Wood, D. F., Williams, T. G., & Mattoso, L. H. C. (2013b). Properties of thermoplastic starch and TPS/polycaprolactone blend reinforced with sisal whiskers using extrusion processing. *Polymer Engineering and Science*, *53*(4), 800–808. https://doi.org/10.1002/pen.23324

Castillo, L. A., López, O. V., García, M. A., Barbosa, S. E., & Villar, M. A. (2019). Crystalline morphology of thermoplastic starch/talc nanocomposites induced by thermal processing. *Heliyon*, *5*(6), e01877. https://doi.org/10.1016/J.HELIYON.2019.E01877

Chang, C., Duan, B., Cai, J., & Zhang, L. (2010). Superabsorbent hydrogels based on cellulose for smart swelling and controllable delivery. *European Polymer Journal*, *46*(1), 92–100. https://doi.org/10.1016/j.eurpolymj.2009.04.033

Chartoff, R., & Sircar, A. (2005). Thermal analysis of polymers. In *Encyclopedia of Polymer Science and Technology* (pp. 1–43).

Chen, J., Wang, X., Long, Z., Wang, S., Zhang, J., & Wang, L. (2020). Preparation and performance of thermoplastic starch and microcrystalline cellulose for packaging composites: Extrusion and hot pressing. *International Journal of Biological Macromolecules*, *165*, 2295–2302. https://doi.org/10.1016/j.ijbiomac.2020.10.117

Ciardelli, F., Bertoldo, M., Bronco, S., & Passaglia, E. (2019). The Obtainment of Bioplastics. In *Polymers from Fossil and Renewable Resources* (pp. 107–132). Springer International Publishing. https://doi.org/10.1007/978-3-319-94434-0_5

Costa, B. P., Carpiné, D., Ikeda, M., Alves, F. E. B. da S., de Melo, A. M., & Ribani, R. H. (2022). Developing a bioactive and biodegradable film from modified loquat (Eriobotrya japonica Lindl) seed starch. *Journal of Thermal Analysis and Calorimetry*, *147*(24), 14297–14313. https://doi.org/10.1007/S10973-022-11780-Z/TABLES/7

Dang, K. M., & Yoksan, R. (2015). Development of thermoplastic starch blown film by incorporating plasticized chitosan. *Carbohydrate Polymers*, *115*, 575–581. https://doi.org/10.1016/J.CARBPOL.2014.09.005

Dang, K. M., & Yoksan, R. (2021). Thermoplastic starch blown films with improved mechanical and barrier properties. *International Journal of Biological Macromolecules*, *188*, 290–299. https://doi.org/10.1016/J.IJBIOMAC.2021.08.027

Enrione, J., Osorio, F., Pedreschi, F., & Hill, S. (2010). Prediction of the Glass Transition Temperature on Extruded Waxy Maize and Rice Starches in Presence of Glycerol. *Food and Bioprocess Technology*, *3*(6), 791–796. https://doi.org/10.1007/S11947-010-0345-1/TABLES/2

European Bioplastics. (2021). *Bioplastics market development*. http://www.european-bioplastics.org/news/publications/

European bioplastics. (2023, May 19). *Bioplastics market development* . Https://Www.European-Bioplastics.Org/Bioplastics-Market-Development-Update-2023-2/.

European Commission. (2022). *European Commission. Commission Regulation (Eu) 2022/1616 of 15 September 2022 on Recycled Plastic Materials and Articles Intended to Come into Contact with Foods, and Repealing Regulation (Ec) No 282/2008 (Text with Eea Relevance)*.

European Commission. (2023). *Single-use plastics*. https://environment.ec.europa.eu/topics/plastics/single-use-plastics_en

Farokhi, M., Jonidi Shariatzadeh, F., Solouk, A., & Mirzadeh, H. (2019). Alginate Based Scaffolds for Cartilage Tissue Engineering: A Review. *Https://Doi.Org/10.1080/00914037.2018.1562924*, *69*(4), 230–247. https://doi.org/10.1080/00914037.2018.1562924

Ferri, J. M., Garcia-Garcia, D., Carbonell-Verdu, A., Fenollar, O., & Balart, R. (2018). Poly(lactic acid) formulations with improved toughness by physical blending with thermoplastic starch. *Journal of Applied Polymer Science*, *135*(4), 45751. https://doi.org/10.1002/app.45751

Foreman, J. (2008). Dynamic Mechanical Analysis of Polymers. In *Encyclopedia of Analytical Chemistry* (Issue January). https://doi.org/10.1002/9780470027318.a2007.pub2

Forssell, P. M., Mikkilä, J. M., Moates, G. K., & Parker, R. (2002). Phase and glass transition behaviour of concentrated barley starch-glycerol-water mixtures, a model for thermoplastic starch. *Carbohydrate Polymers*, *34*(4), 275–282. https://doi.org/10.1016/s0144-8617(97)00133-1

Gadhave, R. V, Das, A., Mahanwar, P. A., & Gadekar, P. T. (2018). Starch Based Bio-Plastics: The Future of Sustainable Packaging. *Open Journal of Polymer Chemistry*, *8*, 21–33. https://doi.org/10.4236/ojpchem.2018.82003

Ghanbari, A., Tabarsa, T., Ashori, A., Shakeri, A., & Mashkour, M. (2018). Preparation and characterization of thermoplastic starch and cellulose nanofibers as green nanocomposites: Extrusion processing. *International Journal of Biological Macromolecules*, *112*, 442–447. https://doi.org/10.1016/j.ijbiomac.2018.02.007

Gopi, S., Balakrishnan, P., Chandradhara, D., Poovathankandy, D., & Thomas, S. (2019). General scenarios of cellulose and its use in the biomedical field. *Materials Today Chemistry*, *13*, 59–78. https://doi.org/10.1016/J.MTCHEM.2019.04.012

Gopi, S., Pius, A., Kargl, R., Kleinschek, K. S., & Thomas, S. (2019). Fabrication of cellulose acetate/chitosan blend films as efficient adsorbent for anionic water pollutants. *Polymer Bulletin*, *76*(3), 1557–1571. https://doi.org/10.1007/S00289-018-2467-Y/TABLES/2

Hambleton, A., Fabra, M. J., Debeaufort, F., Dury-Brun, C., & Voilley, A. (2009). Interface and aroma barrier properties of iota-carrageenan emulsion-based films used for encapsulation of active food compounds. *Journal of Food Engineering*, *93*(1), 80–88. https://doi.org/10.1016/j.jfoodeng.2009.01.001

Hassan, M. M., Le Guen, M. J., Tucker, N., & Parker, K. (2019). Thermo-mechanical, morphological and water absorption properties of thermoplastic starch/cellulose composite foams reinforced with PLA. *Cellulose*, *26*(7), 4463–4478. https://doi.org/10.1007/s10570-019-02393-1

He, Y., Tang, H., Chen, Y., Zhang, S., & Zhang, S. (2020). Facile Strategy to Construct Metal-Organic Coordination Thermoplastic Starch with High Hydrophobicity, Glass-Transition Temperature, and Improved Shape Recovery. *ACS Sustainable Chemistry and Engineering*, *8*(23), 8655–8663.

https://doi.org/10.1021/ACSSUSCHEMENG.0C01579/ASSET/IMAGES/LARGE/SC0C01579_0007.JPEG

Hoffman, A. S. (2012). Hydrogels for biomedical applications. *Advanced Drug Delivery Reviews*, *64*, 18–23. https://doi.org/10.1016/j.addr.2012.09.010

Hoover, R. (2001). Composition, molecular structure, and physicochemical properties of tuber and root starches: a review. *Carbohydrate Polymers*, *45*(3), 253–267. https://doi.org/10.1016/S0144-8617(00)00260-5

Iaccheri, E., Siracusa, V., Ragni, L., De Aguiar Saldanha Pinheiro, A. C., Romani, S., Rocculi, P., Dalla Rosa, M., & Sobral, P. J. do A. (2023). Studying physical state of films based on casava starch and/or chitosan by dielectric and thermal properties and effects of pitanga leaf hydroethanolic extract. *Journal of Food Engineering*, *339*, 111280. https://doi.org/10.1016/J.JFOODENG.2022.111280

International Standards Organization. (2008). *ISO 62:2008 Plastics -- Determination of water absorption.*

International Standards Organization. (2012). *ISO 527-1:2012 - Plastics -- Determination of tensile properties -- Part 1: General principles*. https://doi.org/10.1039/c0cp01060j

International Standards Organization. (2013). *ISO 828:2003-Adhesives. Wettability. Determination by measurement of contact angle and surface free energy of solid surface*.

Ismail, S., Mansor, N., & Man, Z. (2017). A Study on Thermal Behaviour of Thermoplastic Starch Plasticized by [Emim] Ac and by [Emim] Cl. *Procedia Engineering*, *184*, 567–572. https://doi.org/10.1016/j.proeng.2017.04.138

Jiménez, A., Fabra, M. J., Talens, P., & Chiralt, A. (2012). Edible and Biodegradable Starch Films: A Review. *Food and Bioprocess Technology 2012 5:6*, *5*(6), 2058–2076. https://doi.org/10.1007/S11947-012-0835-4

Jumaidin, R., Mohd Zainel, S. N., & Sapuan, S. M. (2020). Processing of Thermoplastic Starch. *Advanced Processing, Properties, and Applications of Starch and Other Bio-Based Polymers*, 11–19. https://doi.org/10.1016/B978-0-12-819661-8.00002-0

Jung, B. N., Kang, D. H., Shim, J. K., & Hwang, S. W. (2019). Physical and mechanical properties of plasticized butenediol vinyl alcohol copolymer/thermoplastic starch blend. *Journal of Vinyl and Additive Technology*, *25*(2), 109–116. https://doi.org/10.1002/vnl.21621

Kaseem, M., Hamad, K., & Deri, F. (2012). Thermoplastic starch blends: A review of recent works. *Polymer Science Series A*, *54*(2), 165–176. https://doi.org/10.1134/s0965545x1202006x

Lendvai, L., Sajó, I., & Karger-Kocsis, J. (2019). Effect of Storage Time on the Structure and Mechanical Properties of Starch/Bentonite Nanocomposites. *Starch - Stärke*, *71*(1–2), 1800123. https://doi.org/10.1002/STAR.201800123

Liu, W. C., Halley, P. J., & Gilbert, R. G. (2010). Mechanism of degradation of starch, a highly branched polymer, during extrusion. *Macromolecules*, *43*(6), 2855–2864. https://doi.org/10.1021/ma100067x

Ma, H., Qin, W., Guo, B., & Li, P. (2022). Effect of plant tannin and glycerol on thermoplastic starch: Mechanical, structural, antimicrobial and biodegradable properties. *Carbohydrate Polymers*, *295*, 119869. https://doi.org/10.1016/J.CARBPOL.2022.119869

Ma, X., & Yu, J. (2004). Formamide as the plasticizer for thermoplastic starch. *Journal of Applied Polymer Science*, *93*(4), 1769–1773. https://doi.org/10.1002/app.20628

Ma, X., Yu, J., He, K., & Wang, N. (2007). The Effects of Different Plasticizers on the Properties of Thermoplastic Starch as Solid Polymer Electrolytes. *Macromolecular Materials and Engineering*, *292*(4), 503–510. https://doi.org/10.1002/MAME.200600445

Marichelvam, Jawaid, & Asim. (2019). Corn and Rice Starch-Based Bio-Plastics as Alternative Packaging Materials. *Fibers*, *7*(4), 32. https://doi.org/10.3390/fib7040032

Mathew, A. P., & Dufresne, A. (2002). Plasticized waxy maize starch: Effect of polyols and relative humidity on material properties. *Biomacromolecules*, *3*(5), 1101–1108. https://doi.org/10.1021/bm020065p

Mendes, J. F., Paschoalin, R. T., Carmona, V. B., Sena Neto, A. R., Marques, A. C. P., Marconcini, J. M., Mattoso, L. H. C., Medeiros, E. S., & Oliveira, J. E. (2016). Biodegradable polymer blends based on corn starch and thermoplastic chitosan processed by extrusion. *Carbohydrate Polymers*, *137*, 452–458. https://doi.org/10.1016/j.carbpol.2015.10.093

Mitrus, M. (2005). Glass transition temperature of thermoplastic starches. *International Agrophysics*, *19*(3), 237–241. http://www.international-agrophysics.org/Glass-transition-temperature-of-thermoplastic-starches,106643,0,2.html

Mitrus, M. (2009). TPS and its nature. In L. P. B. M. Janssen & L. Moscicki (Eds.), *Thermoplastic Starch*. WILEY-VCH Verlag GmbH & Co. KGaA, Weinheim.

Mitrus, M., & Wojtowicz, Agnieszka Moscicki, L. (2009). Biodegradable Polymers and Their Practical Utility. In L. P. B. M. Janssen & L. Moscicki (Eds.), *Thermoplastic Starch*. WILEY-VCH Verlag GmbH & Co. KGaA, Weinheim.

Montilla-Buitrago, C. E., Gómez-López, R. A., Solanilla-Duque, J. F., Serna-Cock, L., & Villada-Castillo, H. S. (2021). Effect of Plasticizers on Properties, Retrogradation, and Processing of Extrusion-Obtained Thermoplastic Starch: A Review. *Starch - Stärke*, *73*(9–10), 2100060. https://doi.org/10.1002/STAR.202100060

Moro, T. M. A., Ascheri, J. L. R., Ortiz, J. A. R., Carvalho, C. W. P., & Meléndez-Arévalo, A. (2017). Bioplastics of Native Starches Reinforced with Passion Fruit Peel. *Food and Bioprocess Technology*, *10*(10), 1798–1808. https://doi.org/10.1007/S11947-017-1944-X/FIGURES/5

Nafchi, A. M., Moradpour, M., Saeidi, M., Alias, A. K., Mohammadi Nafchi, A., Moradpour, M., Saeidi, M., & Alias, A. K. (2013). Thermoplastic starches: Properties, challenges, and prospects. *Starch/Staerke*, *65*(1–2), 61–72. https://doi.org/10.1002/star.201200201

Neus Angles, M., & Dufresne, A. (2000). Plasticized starch/tuniein whiskers nanocomposites. 1. Structural analysis. *Macromolecules*, *33*(22), 8344–8353. https://doi.org/10.1021/ma0008701

Nevoralová, M., Koutný, M., Ujčić, A., Horák, P., Kredatusová, J., Šerá, J., Růžek, L., Růžková, M., Krejčíková, S., Šlouf, M., & Kruliš, Z. (2019). Controlled biodegradability of

functionalized thermoplastic starch based materials. *Polymer Degradation and Stability*, *170*, 108995. https://doi.org/10.1016/J.POLYMDEGRADSTAB.2019.108995

Oniszczuk, T., & Janssen, L. P. B. M. (2009). Influence of Addition of Fiber on the Mechanical Properties of TPS Moldings. In *Thermoplastic Starch*. WILEY-VCH Verlag GmbH & Co. KGaA, Weinheim.

Ostafińska, A., Mikešová, J., Krejčíková, S., Nevoralová, M., Šturcová, A., Zhigunov, A., Michálková, D., & Šlouf, M. (2017). Thermoplastic starch composites with TiO2 particles: Preparation, morphology, rheology and mechanical properties. *International Journal of Biological Macromolecules*, *101*, 273–282. https://doi.org/10.1016/J.IJBIOMAC.2017.03.104

Paiva, D., Pereira, A. M., Pires, A. L., Martins, J., Carvalho, L. H., & Magalhães, F. D. (2018). Reinforcement of thermoplastic corn starch with crosslinked starch/chitosan microparticles. *Polymers*, *10*(9), 985. https://doi.org/10.3390/polym10090985

Paridah, M., Moradbak, A., Mohamed, A. Z., Owolabi, F. abdulwahab taiwo, Asniza, M., & Abdul Khalid, S. H. P. (2016). Thermoplastic Starch. In *Thermoplastic Elastomers*. https://doi.org/http://dx.doi.org/10.5772/57353

Pattanayaiying, R., Sane, A., Photjanataree, P., & Cutter, C. N. (2019). Thermoplastic starch/polybutylene adipate terephthalate film coated with gelatin containing nisin Z and lauric arginate for control of foodborne pathogens associated with chilled and frozen seafood. *International Journal of Food Microbiology*, *290*, 59–67. https://doi.org/10.1016/j.ijfoodmicro.2018.09.015

Pavon, C., Aldas, M., López-Martínez, J., Hernández-Fernández, J., & Patricia Arrieta, M. (2021). Films Based on Thermoplastic Starch Blended with Pine Resin Derivatives for Food Packaging. *Foods*, *10*(6), 1171. https://doi.org/10.3390/foods10061171

Pawlak, A., & Mucha, M. (2003). Thermogravimetric and FTIR studies of chitosan blends. *Thermochimica Acta*, *396*(1–2), 153–166. https://doi.org/10.1016/S0040-6031(02)00523-3

Pushpadass, H. A., Marx, D. B., & Hanna, M. A. (2008). Effects of extrusion temperature and plasticizers on the physical and functional properties of starch films. *Starch/Staerke*, *60*(10), 527–538. https://doi.org/10.1002/star.200800713

Rabe, S., Sanchez-Olivares, G., Pérez-Chávez, R., & Schartel, B. (2019). Natural keratin and coconut fibres from industrial wastes in flame retarded thermoplastic starch biocomposites. *Materials*, *12*(3), 344. https://doi.org/10.3390/ma12030344

Rayón, E., López-Martínez, J., & Arrieta, M. P. (2013). Mechanical characterization of microlaminar structures extracted from cellulosic materials using nanoindentation technique. *Cellulose Chemestry and Technology*, *47*, 345–351. https://www.researchgate.net/publication/258960193_Mechanical_characterization_of_microlaminar_structures_extracted_from_cellulosic_materials_using_nanoindentation_technique

Rodriguez-Gonzalez, F. J., Ramsay, B. A., & Favis, B. D. (2004). Rheological and thermal properties of thermoplastic starch with high glycerol content. *Carbohydrate Polymers*, *58*(2), 139–147. https://doi.org/10.1016/j.carbpol.2004.06.002

Romeira, K. M., Abdalla, G., Gonçalves, R. P., Pegorin, G. S., de Azeredo, H. M. C., Mussagy, C. U., & Herculano, R. D. (2021). Residual Starch Packaging Derived from Potato Washing Slurries to Preserve Fruits. *Food and Bioprocess Technology*, *14*(12), 2248–2259. https://doi.org/10.1007/S11947-021-02694-Z/FIGURES/7

Ruhul Amin, M., Anannya, F. R., Mahmud, M. A., & Raian, S. (2020). Esterification of starch in search of a biodegradable thermoplastic material. *Journal of Polymer Research*, *27*(1), 1–12. https://doi.org/10.1007/S10965-019-1983-2/TABLES/1

Scaffaro, R., Maio, A., & Lopresti, F. (2018). Physical properties of green composites based on poly-lactic acid or Mater-Bi® filled with Posidonia Oceanica leaves. *Composites Part A: Applied Science and Manufacturing*, *112*, 315–327. https://doi.org/10.1016/j.compositesa.2018.06.024

Schmitt, H., Guidez, A., Prashantha, K., Soulestin, J., Lacrampe, M. F., & Krawczak, P. (2015a). Studies on the effect of storage time and plasticizers on the structural variations in thermoplastic starch. *Carbohydrate Polymers*, *115*, 364–372. https://doi.org/10.1016/j.carbpol.2014.09.004

Schmitt, H., Guidez, A., Prashantha, K., Soulestin, J., Lacrampe, M. F., & Krawczak, P. (2015b). Studies on the effect of storage time and plasticizers on the structural variations in thermoplastic starch. *Carbohydrate Polymers*, *115*, 364–372. https://doi.org/10.1016/J.CARBPOL.2014.09.004

Sen, M., Pekel, N., & Gu, O. (1998). Radiation synthesis and characterization of N-vinyl-2-pyrrolidone / N-allylthiourea hydrogels and their use in the adsorption of invertase. *Die Angewandte Makromolekulare Chemie*, *257*(4444), 1–6.

Sessini, V., Arrieta, M. P., Kenny, J. M., & Peponi, L. (2016). Processing of edible films based on nanoreinforced gelatinized starch. *Polymer Degradation and Stability*, *132*, 157–168. https://doi.org/10.1016/j.polymdegradstab.2016.02.026

Sessini, V., Arrieta, M. P., Raquez, J. M., Dubois, P., Kenny, J. M., & Peponi, L. (2019). Thermal and composting degradation of EVA/Thermoplastic starch blends and their nanocomposites. *Polymer Degradation and Stability*, *159*, 184–198. https://doi.org/10.1016/j.polymdegradstab.2018.11.025

Shi, R., Liu, Q., Ding, T., Han, Y., Zhang, L., Chen, D., & Tian, W. (2007). Ageing of Soft thermoplastic Starch with High Glycerol Content. *Journal of Applied Polymer Science*, *103*, 574–586. https://doi.org/10.1002/app

Souza, R. C. R., & Andrade, C. T. (2002a). Investigation of the gelatinization and extrusion processes of corn starch. *Advances in Polymer Technology*, *21*(1), 17–24. https://doi.org/10.1002/adv.10007

Souza, R. C. R., & Andrade, C. T. (2002b). Investigation of the gelatinization and extrusion processes of corn starch. *Advances in Polymer Technology*, *21*(1), 17–24. https://doi.org/10.1002/adv.10007

Stepto, R. F. T. (2006a). Understanding the Processing of Thermoplastic Starch. *Macromolecular Symposia*, *245–246*(1), 571–577. https://doi.org/10.1002/masy.200651382

Stepto, R. F. T. (2006b). Understanding the processing of thermoplastic starch. *Macromolecular Symposia*, *245–246*(1), 571–577. https://doi.org/10.1002/masy.200651382

Taguet, A., Huneault, M. A., & Favis, B. D. (2009). Interface/morphology relationships in polymer blends with thermoplastic starch. *Polymer*, *50*(24), 5733–5743. https://doi.org/10.1016/j.polymer.2009.09.055

Teixeira, E. de M., Curvelo, A. A. S., Corrêa, A. C., Marconcini, J. M., Glenn, G. M., & Mattoso, L. H. C. (2012). Properties of thermoplastic starch from cassava bagasse and cassava starch and their blends with poly (lactic acid). *Industrial Crops and Products*, *37*(1), 61–68. https://doi.org/10.1016/j.indcrop.2011.11.036

Thuwall, M., Boldizar, A., & Rigdahl, M. (2006). Extrusion processing of high amylose potato starch materials. *Carbohydrate Polymers*, *65*(4), 441–446.

Toro-Márquez, L. A., Merino, D., & Gutiérrez, T. J. (2018). Bionanocomposite Films Prepared from Corn Starch With and Without Nanopackaged Jamaica (Hibiscus sabdariffa) Flower Extract. *Food and Bioprocess Technology*, *11*(11), 1955–1973. https://doi.org/10.1007/S11947-018-2160-Z/FIGURES/7

Van Soest, J. J. G., De Wit, D., & Vliegenthart, J. F. G. (1996). Mechanical properties of thermoplastic waxy maize starch. *Journal of Applied Polymer Science*, *61*(11), 1927–1937. https://doi.org/10.1002/(sici)1097-4628(19960912)61:11<1927::aid-app7>3.0.co;2-l

Vinod, A., Sanjay, M. R., Suchart, S., & Jyotishkumar, P. (2020). Renewable and sustainable biobased materials: An assessment on biofibers, biofilms, biopolymers and biocomposites. *Journal of Cleaner Production*, *258*, 120978. https://doi.org/10.1016/J.JCLEPRO.2020.120978

Wang, H.-Y., & Huang, M. (2007a). Preparation, characterization and performances of biodegradable thermoplastic starch. *Polymers for Advanced Technologies*, *18*(April), 910–915. https://doi.org/10.1002/pat

Wang, H.-Y., & Huang, M. (2007b). Preparation, characterization and performances of biodegradable thermoplastic starch. *Polymers for Advanced Technologies*, *18*(April), 910–915. https://doi.org/10.1002/pat

Wattanakornsiri, A., Pachana, K., Kaewpirom, S., Traina, M., & Migliaresi, C. (2012). Preparation and Properties of Green Composites Based on Tapioca Starch and Differently Recycled Paper Cellulose Fibers. *Journal of Polymers and the Environment*, *20*(3), 801–809. https://doi.org/10.1007/s10924-012-0494-6

Wilpiszewska, K., & Spychaj, T. (2006). Heat plasticization of starch by extrusion in the presence of plasticizers. *Polimery*, *51*(05), 327–332. https://doi.org/10.14314/polimery.2006.327

Xie, F., Halley, P. J., & Avérous, L. (2012). Rheology to understand and optimize processibility, structures and properties of starch polymeric materials. *Progress in Polymer Science (Oxford)*, *37*(4), 595–623. https://doi.org/10.1016/j.progpolymsci.2011.07.002

Xie, F., Luckman, P., Milne, J., McDonald, L., Young, C., Tu, C. Y., di Pasquale, T., Faveere, R., & Halley, P. J. (2014). Thermoplastic starch: Current development and future trends. *Journal of Renewable Materials*, *2*(2), 95–106. https://doi.org/10.7569/JRM.2014.634104

Yang, J. H., Yu, J. G., & Ma, X. F. (2006). A novel plasticizer for the preparation of thermoplastic starch. *Chinese Chemical Letters*, *17*(1), 133–136.

Ye, J., Hu, X., Luo, S., Liu, W., Chen, J., Zeng, Z., & Liu, C. (2018). Properties of Starch after Extrusion: A Review. *Starch - Stärke*, *70*(11–12), 1700110. https://doi.org/10.1002/STAR.201700110

Yunos, M. Z. B., & Rahman, W. A. W. A. (2011). Effect of Glycerol on Performance Rice Straw/Starch Based Polymer. *Journal of Applied Sciences*, *11*(13), 2456–2459.

Zhang, X., Ma, H., Qin, W., Guo, B., & Li, P. (2022). Antimicrobial and improved performance of biodegradable thermoplastic starch by using natural rosin to replace part of glycerol. *Industrial Crops and Products*, *178*, 114613. https://doi.org/10.1016/J.INDCROP.2022.114613

Zhang, Y., Rempel, C., & Liu, Q. (2014). Thermoplastic Starch Processing and Characteristics-A Review. *Critical Reviews in Food Science and Nutrition*, *54*(10), 1353–1370. https://doi.org/10.1080/10408398.2011.636156

Zhang, Y., Rempel, C., & McLaren, D. (2014). Thermoplastic Starch. In *Innovations in Food Packaging* (pp. 391–412). Academic Press. https://doi.org/10.1016/B978-0-12-394601-0.00016-3

Zhong, Q., Gao, B., Weng, Y., & Zhang, S. (2022). Adopting Intrinsic Hydrophilic Thermoplastic Starch Composites to Fabricate Antifogging Sustainable Films with High Antibiosis and Transparency. *ACS Sustainable Chemistry and Engineering*, *10*(11), 3661–3672. https://doi.org/10.1021/ACSSUSCHEMENG.1C08660/SUPPL_FILE/SC1C08660_SI_002.MP4

Zullo, R., & Iannace, S. (2009). The effects of different starch sources and plasticizers on film blowing of thermoplastic starch: Correlation among process, elongational properties and macromolecular structure. *Carbohydrate Polymers*, *77*(2), 376–383. https://doi.org/10.1016/j.carbpol.2009.01.007